National Library
of Canada

Canadian Theses Service

Ottawa, Canada
K1A 0N4

Bibliothèque nationale
du Canada

Services des thèses canadiennes

CANADIAN THESES

THÈSES CANADIENNES

NOTICE

The quality of this microfiche is heavily dependent upon the quality of the original thesis submitted for microfilming. Every effort has been made to ensure the highest quality of reproduction possible.

If pages are missing, contact the university which granted the degree.

Some pages may have indistinct print especially if the original pages were typed with a poor typewriter ribbon or if the university sent us an inferior photocopy.

Previously copyrighted materials (journal articles, published tests, etc.) are not filmed.

Reproduction in full or in part of this film is governed by the Canadian Copyright Act, R.S.C. 1970, c. C-30. Please read the authorization forms which accompany this thesis.

AVIS

La qualité de cette microfiche dépend grandement de la qualité de la thèse soumise au microfilmage. Nous avons tout fait pour assurer une qualité supérieure de reproduction.

S'il manque des pages, veuillez communiquer avec l'université qui a conféré le grade.

La qualité d'impression de certaines pages peut laisser à désirer, surtout si les pages originales ont été dactylographiées à l'aide d'un ruban usé ou si l'université nous a fait parvenir une photocopie de qualité inférieure.

Les documents qui font déjà l'objet d'un droit d'auteur (articles de revue, examens publiés, etc.) ne sont pas microfilmés.

La reproduction, même partielle, de ce microfilm est soumise à la Loi canadienne sur le droit d'auteur, SRC 1970, c. C-30. Veuillez prendre connaissance des formules d'autorisation qui accompagnent cette thèse.

THIS DISSERTATION
HAS BEEN MICROFILMED
EXACTLY AS RECEIVED

LA THÈSE A ÉTÉ
MICROFILMÉE TELLE QUE
NOUS L'AVONS REÇUE

NL 339 (r. 86/01)

Canada

354

0-315-27085-3

National Library of Canada
Bibliothèque nationale du Canada

Canadian Theses Division
Division des thèses canadiennes

Ottawa, Canada
K1A 0N4

PERMISSION TO MICROFILM — AUTORISATION DE MICROFILMER

- Please print or type — Écrire en lettres moulées ou dactylographier

Full Name of Author — Nom complet de l'auteur
IQBAL HUSSEIN · AHMED

Date of Birth — Date de naissance
30 | 12 | 1953

Country of Birth — Lieu de naissance
UGANDA

Permanent Address — Résidence fixe
41, SOMERSET HOUSE
SOMERSET ROAD
LONDON SW19 5JA

Title of Thesis — Titre de la thèse
PULMONARY PERMEABILITY IN RADIATION LUNG INJURY

University — Université
ALBERTA

Degree for which thesis was presented — Grade pour lequel cette thèse fut présentée
MSc

Year this degree conferred — Année d'obtention de ce grade
1984

Name of Supervisor — Nom du directeur de thèse
DR PAUL MAN

Permission is hereby granted to the NATIONAL LIBRARY OF CANADA to microfilm this thesis and to lend or sell copies of the film.

The author reserves other publication rights, and neither the thesis nor extensive extracts from it may be printed or otherwise reproduced without the author's written permission.

L'autorisation est, par la présente, accordée à la BIBLIOTHÈQUE NATIONALE DU CANADA de microfilmer cette thèse et de prêter ou de vendre des exemplaires du film.

L'auteur se réserve les autres droits de publication; ni la thèse ni de longs extraits de celle-ci ne doivent être imprimés ou autrement reproduits sans l'autorisation écrite de l'auteur.

Date
24/4/84.

Signature
Iqbal Ahmed

NL-91 (4/77)

THE UNIVERSITY OF ALBERTA

PULMONARY PERMEABILITY
IN RADIATION LUNG INJURY

by

© IQBAL HUSSEIN AHMED

A THESIS

SUBMITTED TO THE FACULTY OF GRADUATE STUDIES
AND RESEARCH IN PARTIAL FULFILMENT OF THE
REQUIREMENTS FOR THE DEGREE OF
MASTER OF SCIENCE
IN
EXPERIMENTAL MEDICINE

DEPARTMENT OF MEDICINE

EDMONTON, ALBERTA
SPRING, 1984

founded 1892

The
Children's Hospital
of Buffalo

219 Bryant Street, Buffalo, New York 14222
716 878-7000

February 23, 1984

Iqbal H. Ahmed, M.B., MRCP (U.K.)
Department of Medicine
Clinical Sciences Building
The University of Alberta
Edmonton, Alberta T6G 2G3

Dear Sir or Madam:

You have my permission to use the following illustration(s) in the literature review section of your thesis entitled "Alveolar-capillary membrane permeability in radiation lung injury":

> "Response of alveolar epithelial solute permeability to changes in lung inflation." Journal of Applied Physiology 1980; 49: 1035. Fig. 2
>
> "Lung inflation and alveolar permeability to non-electrolytes in adult sheep in vivo". J. Physiol. (Lond) 1976; 260: page 414, Fig. 1 and page 420, Fig. 6.

Sincerely,

EAEgan, MD/dg

Edmund A. Egan, MD
Professor of Pediatrics
State Univ. of NY at Buffalo
Head, Newborn Medicine
Children's Hospital of Buffalo

dg

AN AFFILIATED TEACHING HOSPITAL OF THE HEALTH SCIENCE SCHOOLS OF THE STATE UNIVERSITY OF NEW YORK AT BUFFALO

THE PHYSIOLOGICAL SOCIETY

Professor R. J. Linden
Honorary Treasurer

Department of Cardiovascular Studies
University of Leeds
Leeds LS2 9JT

Tel. Leeds (0532) 452088

3 January 1984

Dr I H Ahmed
Department of Medicine
Clinical Sciences Building
The University of Alberta
Edmonton
Alberta
Canada T6G 2G3

Dear Dr Ahmed

Thank you for your letter of 5 December 1983 requesting permission to reproduce the following material:

Fig 1 and Fig 6 from J Physiol (1976), 260: 414-420.

The Physiological Society is happy to grant you permission, provided the consent of the authors is first obtained.

Yours sincerely

CHPatrick

pp R J Linden
Honorary Treasurer

UNIVERSITY OF MEDICINE AND DENTISTRY OF NEW JERSEY
100 BERGEN STREET / NEWARK, NEW JERSEY 07103

February 22, 1984

Igbal H. Ahmed, M.B., MRCP (U.K.)
Department of Medicine
Clinical Sciences Building
The University of Alberta
Edmonton, Alberta
T6G 2G3

Dear Sir:

In response to your recent request, I gladly permit you to use Figue I in my article, "Ultrastructural features of alveolar epithelial transport", Am. Rev. Resp. Dis. 1983 in the literature review section of your thesis.

I wish you luck with your work and judging by the title of your thesis, your results should prove to be most interesting.

Sincerely,

David O. DeFouw, Ph.D.
Department of Anatomy

DDF/e

With reference to your letter of 5th December,

The Macmillan Press Limited grant permission for reproduction of the following material:
Fig. 7 p. 714 in 'The physiology of leaky lungs' - J.G. Jones, B.D. Minty and D. Royston, British Journal of Anaesthesia (1982).

This permission is granted to the person named below for the purpose specified below:

Mr Iqbal H. Ahmed
Clinical Sciences Building
Department of Medicine
The University of Alberta
Edmonton
Alberta
Canada T6G 2G3

Figure to be included in thesis entitled 'Alveolar-capillary membrane permeability in radiation lung injury' for MSc degree at the University of Alberta, Edmonton, Canada.

and is subject to the following conditions:

(a) the source of the material is acknowledged by a full reference to the original article.

(b) permission to reproduce the material is obtained from the author(s) of the original article

Signed....Mrs. M. White.......... Date....6 January 1984....
Permissions Executive

Scientific & Medical Division
The Macmillan Press Ltd
Houndmills Basingstoke Hampshire RG21 2XS Telephone Basingstoke 29242 (STD Code 0256) Cables Publish Basingstoke Telex 858493
Registered Office 4 Little Essex Street London WC2R 3LF Registered No. 994011 England

DEPARTMENT OF MEDICINE

CLINICAL SCIENCES BUILDING
THE UNIVERSITY OF ALBERTA
EDMONTON, ALBERTA
T6G 2G3

The Editor,
The American Physiological Society
9650 Rockville Pike
Bethesda, MD 20014
USA

December 5, 1983

Dear Sir:

I am preparing a thesis entitled "Alveolar-capillary membrane permeability in radiation lung injury" for the degree of MSc at the University of Alberta, Edmonton, Canada.

I would like to request permission to use the following illustration(s) in the literature review section of this thesis:

1032-1036 Response of alveolar epithelial solute permeability to changes in lung inflation. E.A. Egan, JAP, 1980; 49, Fig.2, page 1035.

I would appreciate your early reply,

Yours sincerely,

Iqbal H. Ahmed, M.B.,MRCP(U.K.)

IA/dmb

AMERICAN PHYSIOLOGICAL SOCIETY
DEC 15 1983

THE AMERICAN PHYSIOLOGICAL SOCIETY
9650 Rockville Pike — Bethesda, MD 20014

Permission is granted for use of the material specified above, contingent upon consent of the author and provided the publication is credited as the source.

12-20-83
Date

S.R. Geiger
Stephen R. Geiger
Publ Mgr & Exec Editor

DEPARTMENT OF MEDICINE

CLINICAL SCIENCES BUILDING
THE UNIVERSITY OF ALBERTA
EDMONTON, ALBERTA
T6G 2G3

The Editor,
Microvascular Research
111 Fifth Avenue
New York, N.Y. 10003
USA

DEC 16 1983

December 5, 1983

Dear Sir:

I am preparing a thesis entitled "Alveolar-capillary membrane permeability in radiation lung injury" for the degree of MSc at the University of Alberta, Edmonton, Canada.

I would like to request permission to use the following illustration(s) in the literature review section of this thesis:

> The alveolar-capillary barrier: some data and speculations. 1980, 19, Fig.2, page 5.

I would appreciate your early reply,

Yours sincerely,

Iqbal H. Ahmed, M.B.,MRCP(U.K.)

IA/dmb

PERMISSION GRANTED, provided that complete credit is given to original publication in our book.

12/19/83

M. McGrath
Marian McGrath
Rights & Permissions
Academic Press, Inc.

Please pardon the informality but to speed our reply we have answered on your own letter.

DEPARTMENT OF MEDICINE

CLINICAL SCIENCES BUILDING
THE UNIVERSITY OF ALBERTA
EDMONTON, ALBERTA
T6G 2G3

The Editor,
American Review of Respiratory Disease
2850 N. Charles Street
Baltimore, MD 21218
USA

December 5, 1983

Dear Sir:

I am preparing a thesis entitled "Alveolar-capillary membrane permeability in radiation lung injury" for the degree of MSc at the University of Alberta, Edmonton, Canada.

I would like to request permission to use the following illustration(s) in the literature review section of this thesis:

(1) Ultrastructural features of alveolar epithelial transport. David D. Defouw, 127 supp., Fig.1, page s10.

(2) Measurements of pulmonary epithelial permeability in vivo. R.M. Effros and G.R. Mason, 127 supp, Fig.1, page S63.

I would appreciate your early reply,

Yours sincerely,

Iqbal H. Ahmed, M.B.,MRCP(U.K.)

IA/dmb

PERMISSION GRANTED PROVIDED YOU CREDIT
THE AMERICAN REVIEW OF RESPIRATORY DISEASE.
IF THE ARTICLE WAS PUBLISHED BEFORE 1979 --
PERMISSION OF THE AUTHOR(S) IS ALSO NECESSARY.
AUTHOR(S) ADDRESS IS FOOTNOTED TO PRINTED ARTICLE.

Mary Thornton 12/20/83
Mary J. Thornton
Assistant Editor
Date

DEPARTMENT OF MEDICINE

CLINICAL SCIENCES BUILDING
THE UNIVERSITY OF ALBERTA
EDMONTON, ALBERTA
T6G 2G3

The Editor,
Federation of American Societies
for Experimental Biology
9650 Rockville Pike
Bethesda, MD 20014
USA

FASEB
DEC 15 1983
PUBLICATIONS

December 5, 1983

Dear Sir:

I am preparing a thesis entitled "Alveolar-capillary membrane permeability in radiation lung injury" for the degree of MSc at the University of Alberta, Edmonton, Canada.

I would like to request permission to use the following illustration(s) in the literature review section of this thesis:

> Structural basis for some permeability properties of the air-blood barrier. Federation Proceedings, 1978; 37, Fig.6, page 2476.

I would appreciate your early reply,

Yours sincerely,

Iqbal H. Ahmed, M.B.,MRCP(U.K.)

IA/dmb

27 December 1983 Permission granted for the above request. Please give credit to Federation Proceedings.

Judith B Gandy

Judith B. Gandy
Assistant Executive Editor

British Journal of Anaesthesia

EDITOR OF GENERAL ISSUES:
WILLIAM FITCH BSc, MB, ChB, PhD, FFARCS,
University Department of Anaesthesia, Glasgow Royal Infirmary,
Glasgow, G31 2ER. Telephone: 041-552 3535, ext. 5446

EDITOR OF EDUCATIONAL ISSUES:
GRAHAM SMITH Bsc, MD, FFARCS, Professor of Anaesthesia,
University Department of Anaesthesia, Leicester Royal Infirmary,
Leicester, LE1 5WW,
Telephone: 0533 541414, ext. 5291

WF/IMcM

20th December, 1983.

Dr. Iqbal H. Ahmed
Department of Medicine
Clinical Sciences Building
The University of Alberta
Edmonton
Alberta T6G 2G3
CANADA

Dear Dr. Ahmed,

Thank you for your letter requesting permission to use illustrations previously published in BJA. I have pleasure in affording permission on the understanding that due acknowledgement will be made to the source of the material, and that you have also obtained the permission of the authors of the article to reproduce their material.

The physiology of leaky lungs.
J.G. Jones, B.D. Minty and D. Royston
1982, 54, Fig. 7, page 714

Yours sincerely,

William Fitch

WILLIAM FITCH
Editor

The Macmillan Press Ltd., Registered Office: 4 Little Essex Street, London WC2R 3LF, Registered No. 994011 England

UNIVERSITY OF CALIFORNIA, LOS ANGELES

BERKELEY · DAVIS · IRVINE · LOS ANGELES · RIVERSIDE · SAN DIEGO · SAN FRANCISCO · SANTA BARBARA · SANTA CRUZ

1868

DEPARTMENT OF PHYSIOLOGY
SCHOOL OF MEDICINE
THE CENTER FOR THE HEALTH SCIENCES
LOS ANGELES, CALIFORNIA 90024

February 22, 1984

Iqbal H. Ahmed, M.B.
Department of Medicine
Clinical Sciences Building
The University of Alberta
Edmonton, Alberta T6G 2G3
CANADA

Dear Dr. Ahmed,

Of course you have my permission. I would like a copy of your thesis when it is finished.

My address from April this year will be:

Niels Bindslev, M.D.
Department of Medical Physiology, A
Panum Institute
2200 Copenhagen N
Denmark

Sincerely yours,

Niels Bindslev

Niels Bindslev, M.D.

NB:bw

DEPARTMENT OF MEDICINE

CLINICAL SCIENCES BUILDING
THE UNIVERSITY OF ALBERTA
EDMONTON, ALBERTA
T6G 2G3

Dr. R.M. Effros
Division of Respiratory Physiology
and Medicine
Harbor-UCLA Medical Centre
Torrance, California
USA

December 5, 1983

Dear Sir:

I am preparing a thesis entitled "Alveolar-capillary membrane permeability in radiation lung injury" for the degree of MSc at the University of Alberta, Edmonton, Canada.

I would like to request permission to use the following illustration(s) in the literature review section of this thesis:

> "Measurements of pulmonary epithelial permeability in vivo". Am. Rev. Respir. Dis. 1983; 127 supp, 563, Fig.1

I would appreciate your early reply,

Yours sincerely,

Iqbal H. Ahmed, M.B.,MRCP(U.K.)

IA/dmb

2/21/84

Dear Dr. Ahmed
Permission is granted for use
of this figure in your thesis
R. Effros

Medical Research Council
Clinical Research Centre
In association with
Northwick Park Hospital
Harrow Health Authority

CLINICAL RESEARCH CENTRE
DIVISION OF ANAESTHESIA
Watford Road, Harrow, Middlesex HA1 3UJ
telephone: 01-864 5311 ext
telex: 923410

27th February, 1984

JGJ/ns

Dr. Iqbel H. Ahmed,
Department of Medicine,
Clinical Sciences Building,
The University of Alberta,
Edmonton,
Alberta T6G 2G3.

Dear Dr. Ahmed,

Thank you for your letter. I am delighted for you to use the Fig. 7 in British Journal of Anaesthesia, 54, 1982, in your thesis. I would be most interested to hear of your findings.

Yours sincerely,

J.G. Jones

THE UNIVERSITY OF ALBERTA

RELEASE FORM

NAME OF AUTHOR - Iqbal Hussein Ahmed

TITLE OF THESIS - Pulmonary permeability in radiation lung injury

DEGREE FOR WHICH THESIS WAS PRESENTED - MSc

YEAR THIS DEGREE GRANTED - 1984

Permission is hereby granted to THE UNIVERSITY OF ALBERTA LIBRARY to reproduce single copies of this thesis and to lend or sell such copies for private, scholarly or scientific research purposes only.

The author reserves other publication rights, and neither the thesis nor extensive extracts from it may be printed or otherwise reproduced without the author's written permission.

....

PERMANENT ADDRESS

41 Somerset House
Somerset Road
London SW19 5JA
ENGLAND

DATED 24/4/84

THE UNIVERSITY OF ALBERTA

FACULTY OF GRADUATE STUDIES AND RESEARCH

The undersigned certify that they have read, and recommend to the Faculty of Graduate Studies and Research, for acceptance, a thesis entitled Pulmonary permeability in radiation lung injury submitted by Iqbal Hussein Ahmed in partial fulfilment of the requirements for the degree of Master of Science in Experimental Medicine.

....

Supervisor

....

Theodor K. Shnitka

J. Battista

Godfrey Man

Date 13/4/84

ABSTRACT

Ultrastructural studies of the alveolar-capillary membrane show that changes which may alter its permeability characteristics are an early and consistent feature of radiation lung injury. To assess changes in pulmonary permeability at weekly intervals following thoracic irradiation (20 Gy rad to a 5 X 7 cm area in the right lower zone) in 12 dogs, we measured the regional pulmonary clearance rates of aerosolized sodium pertechnetate (TcO_4^-) and technetium-labeled diethylenetriaminepenta-acetate (DTPA). Chest roentgenograms (Cxray) and ^{99m}Tc-macroaggregated albumin (MAA) perfusion scans were also performed weekly and computerized tomographic (CT) lung scans biweekly for comparison. Dogs were sacrificed at the end of the study for lung compliance measurements and morphology. Before irradiation there were no side to side differences in pulmonary clearance rates of the solutes; for TcO_4, right = 4.19 ± 0.72 min, left = 4.33 ± 0.71 min ($t\frac{1}{2}$, mean ± SD); for DTPA, right = 2.99 ± 0.74 %/min, left = 3.3 ± 0.98 %/min (% fall per min, mean ± SD). Following irradiation, pulmonary clearance rates of both solutes were reduced on the irradiated side and these were statistically different from those of the non-irradiated side from the second week onwards. Cxray, MAA and CT scans did not become abnormal until much later 8.22 ± 2.64, 8.0 ± 3.08 and 7.11 ± 2.76 weeks post-irradiation respectively (mean ± SD). At autopsy, all dogs showed histological evidence of radiation

pneumonitis but the compliance of excised right lower lobes was not altered. However two separate dogs sacrificed at the onset of abnormal TcO_4^- clearance showed normal lung histology. These results indicate that pulmonary permeability is reduced in experimental radiation lung injury and that this occurs before widespread morphological, radiological and perfusion abnormalities become detectable. Therefore the radioaerosol scanning technique which can detect regional changes in pulmonary permeability has potential value in the early detection of radiation lung injury.

ACKNOWLEDGEMENTS

I would like to express my sincere gratitude to my supervisor, Dr. Paul Man, for his continued guidance, encouragement and support during this project. The assistance of my advisors, Dr. Godfrey Man, Dr. Jerry Battista, Dr. Brian Sproule and Dr. T. Shnitka is also gratefully acknowledged.

Special thanks go to Dr. Helen Ferri for the interpretation of the CT scans, Dr. John Jacques for assistance with the lung morphology, Dr. Gerry Hill for advice on statistical analyses, and Dianne Benwood for excellent secretarial assistance.

The project certainly owes a great deal to Wayne Logus, Ellen El-Khatib, Helen Herklotz, Hans Yamamoto and Rick Volpel for their technical expertise in various matters and to them I am deeply indebted.

I would like to express my sincere appreciation to the staff of the Surgical-Medical Research Institute, University of Alberta and the W.W. Cross Cancer Institute, Edmonton for the use of their facilities.

Finally I acknowledge with deep gratitude the Alberta Heritage Foundation for Medical Research for their generous Fellowship award, and support for the project from their Applied Cancer Research Fund.

TABLE OF CONTENTS

CHAPTER PAGE

I THE PROBLEM 1

(i) BACKGROUND TO THE PROBLEM 2

(ii) STATEMENT OF THE PROBLEM 4

(iii) RESEARCH HYPOTHESIS 6

(iv) OBJECTIVES OF THE STUDY . 7

II A REVIEW OF THE LITERATURE 8

(i) INTRODUCTION 9

(ii) ULTRASTRUCTURE OF THE ALVEOLAR-CAPILLARY MEMBRANE 10

(iii) INTERCELLULAR JUNCTIONS 17

(iv) PATHWAYS FOR SOLUTE AND FLUID PERMEATION 21

(v) METHODS OF MEASURING ALVEOLAR-CAPILLARY MEMBRANE PERMEABILITY 30

(vi) ALTERATIONS IN PULMONARY PERMEABILITY 41

(vii) RADIATION LUNG INJURY 48

III EXPERIMENTAL 56

(i) SUMMARY OF PROTOCOL 57

(ii) PRE-IRRADIATION RADIOAEROSOL SCANNING 58

(iii) CONVENTIONAL PRE-IRRADIATION IMAGING 64

(iv) IRRADIATION 66

(v) POST-IRRADIATION IMAGING 67

CHAPTER PAGE

III EXPERIMENTAL (cont'd)

(vi) MEASUREMENT OF LOBAR COMPLIANCE 69
(vii) MORPHOLOGY 70
IV RESULTS 71
V DISCUSSION 92
VI SUMMARY AND CONCLUSIONS 110

* * *

REFERENCES 112
APPENDIX 1 - CALCULATION OF RADIATION TREATMENT TIMES 128
APPENDIX 2 - BLOOD BACKGROUND (R_B) AFTER IRRADIATION 129
APPENDIX 3 - SUMMARY OF TcO_4^- DATA 131
APPENDIX 4 - SUMMARY OF DTPA DATA 133
APPENDIX 5 - CURRICULUM VITA 135

LIST OF TABLES

TABLE	DESCRIPTION	PAGE
1	Species differences in half time clearance from lung to blood (T ½ LB).	40
2	Morphological lung changes after thoracic irradiation.	51
3	Ventilation parameters during aerosolization.	73
4	Confidence limits for TcO_4^- clearance (t ½) and the time of onset of abnormality	77
5	Mean CT number for the right lower zone at various time intervals after irradiation.	80
6	Changes in regional MAA count ratios after irradiation and the onset of abnormality.	83
7	The onset of abnormality in various tests following thoracic irradiation.	84
8	Compliance (Kc) of the right and left lower lobes after right lower zone thoracic irradiation.	86

LIST OF FIGURES

FIGURE	DESCRIPTION	PAGE
1	Relationship between solute clearance and molecular weight.	14
2	Experimental relationship between permeability coefficients and partition coefficients for the toad urinary bladder.	22
3	A diagrammatic representation of the alveolar-capillary membrane.	23
4	Typical curves obtained from a multiple indicator-dilution experiment in which ^{14}C-butanediol is the test substance and T-1824 the vascular (impermeant) tracer.	31
5	Relationship of the change in concentration of solutes in alveolar saline with time.	34
6	Sequential arterial blood samples analyzed for ^{51}Cr EDTA and ^{125}I antipyrine immediately after injecting a bolus of the two tracers into the airway.	36

LIST OF FIGURES

FIGURE	DESCRIPTION	PAGE
7	Relationship between lung inflation and calculated alveolar epithelial pore radius in adult sheep in vivo.	42
8	Relationship between inflation volume and alveolar epithelial pore radius in consecutive inflations in adult dogs.	43
9	The experimental circuit showing a dog positioned under the gamma camera and the aerosol generation system of nebulizer and reservoir bag.	60
10	Determination of blood background.	63
11	Changes in the lung clearance of TcO_4^- (t ½) for the right and left lower zones following thoracic irradiation.	75
12	Changes in the lung clearance of TcO_4^- (t ½) for the right and left lower zones following right lower zone irradiation in dog C-620.	76

LIST OF FIGURES

FIGURE	DESCRIPTION	PAGE
13	Changes in lung clearance of DTPA (k%/min) for the right and left lower zones following right lower zone thoracic irradiation.	78
14	Changes in average CT number in the right lower zone after irradiation in 10 dogs.	82

LIST OF PHOTOGRAPHIC PLATES

PLATE	DESCRIPTION	PAGE
1.	An example of the alveolar-capillary membrane from an isolated perfused dog lung after perfusion-fixation.	11
2.	Excised right lower lobe after thoracic irradiation showing obvious scarring.	87
3.	Changes in light microscopy in the right lower lobe in dog C-620.	88
4.	Section from left lower lobe of dog C-620 showing normal histology.	89
5.	Section from the right lower lobe of an early sacrifice dog showing normal histology.	91

CHAPTER I

THE PROBLEM

Background to the problem

Radiation treatment is an effective modality in the management of malignancy. Its ability to reduce tumour mass and relieve symptoms has been demonstrated in a wide variety of cancers, both primary and secondary. Despite this usefulness a major limitation has been its inability to discriminate between healthy and malignant tissue. In treatment schedules to the thorax, for instance, the effect of radiation on the lungs has been the major limiting factor. Since the first reports of radiation lung injury in 1922, from Groover, Christie and Merritt,(1) many of the factors in its pathogenesis have been elucidated. Thus, it is now possible by using dose fractionation, the avoidance of exacerbating factors, and improving dose distributions to reduce the toxic effects of radiation on normal lung tissue. Nevertheless, radiation lung injury still occurs with significant morbidity and mortality.(2) In addition there is considerable variability in response between patients on the same radiation therapy protocol. It is therefore difficult to determine a priore or during treatment who will and who will not develop a severe reaction. Two syndromes have been described: radiation pneumonitis, an exudative lung reaction occurring acutely 3-6 months after irradiation; and radiation fibrosis, a "healing" reaction occurring months or even years later. Although far less common than fibrosis, radiation pneumonitis accounts for most of the morbidity and mortality seen in radiation lung injury. At the present time its diagnosis is based largely upon symptomatology and chest radiography. Steroids, antibiotics and anticoagulants have all been used in the management of pneumonitis.(3) Of these three, steroid treatment has been the only one which has shown any benefit in animal studies.(3) Although there are anecdotal reports of benefit in humans(4) there have been no controlled clinical trials and most physicians favour supportive therapy alone.

It is clear, therefore, that despite its usefulness both alone and in combination with chemotherapy and surgery, the effectiveness of radiation treatment in the management of cancer is compromised by the need to consider or reverse its effects on normal tissue.

Statement of the problem

Although the clinical and radiographic features of radiation pneumonitis do not appear until 3-6 months after irradiation it is likely that lung damage is almost immediate.(5-11) Indeed ultrastructural studies have shown changes within the first 24-48 hours in rats given 20 Gy to the left chest.(5) A latent interval therefore exists between irradiation and the onset of symptoms and radiographic abnormalities. During this interval the ultrastructural changes either progress to produce an exudative reaction (radiation pneumonitis) or heal, leading to fibrous scarring (radiation fibrosis). The factors which influence the direction the lung injury takes have not been fully established although radiation parameters (e.g. dose and volume) are important. The early changes seem to be centered upon the alveolar epithelium and/or the capillary endothelium with initial swelling and eventual sloughing of cells. Clearly whatever mechanisms are responsible, their effects persist during the latent interval. At the present time, no non-invasive method exists to adequately assess this early damage. Moreover, in the clinical setting, repeated lung biopsies during this interval would be clearly impractical. By the time symptoms and radiographic abnormalities develop, it is often too late for effective intervention. A non-invasive test is required to detect early changes, to predict the likelihood of developing pneumonitis, and to assess the effectiveness of intervention. Such a test could be used to follow patients during and after radiotherapy and to help optimize this potent treatment modality.

Research Hypothesis

The early damage following radiation therapy is centered upon the alveolar epithelium and capillary endothelium.(5-11) As these two linings make up the major components of the alveolar-capillary membrane(12) it is postulated that damage to them alters its permeability characteristics. A non-invasive assessment of pulmonary permeability following radiation therapy may therefore provide a test which can be used to monitor damage in patients after radiation treatment. If changes in pulmonary permeability occur early this test may be able to identify damage earlier than chest radiography, tomography or clinical examination. It is also possible that this alteration in barrier properties is an important early step in the pathogenesis of radiation pneumonitis and its assessment may provide further clues as to the chain of events that follow.

Objectives of the study

The objectives of this study were as follows:

(1) To document changes in pulmonary permeability in vivo following thoracic irradiation in dogs, using a radioaerosol scanning procedure.

(2) To identify the time of onset of these changes by serial assessment of pulmonary permeability after irradiation.

(3) To determine the value of this test in the early detection of radiation lung injury by comparison with serial chest radiographs, ^{99m}Technetium labeled macroaggregated albumin (MAA) perfusion and x-ray computerized tomographic (CT) lung scans.

(4) To document the degree of radiation damage produced by the measurement of the compliance of irradiated lobes and morphological examination of the lungs.

CHAPTER II

A REVIEW OF THE LITERATURE

Introduction

In order to fully comprehend the effects of radiation on pulmonary permeability, it is important to have a basic understanding of the air-blood barrier and its permeability characteristics. In the literature review which follows, therefore, the alveolar-capillary membrane is considered in some depth. Many reviews of radiation lung injury already exist,(2,13) and for the purposes of this thesis, only the effects of radiation on the alveolar-capillary membrane will be considered. Throughout this literature review emphasis has been placed on what is relevant to the experimental section and to the objectives of the study.

Ultrastructure of the alveolar-capillary membrane

The alveolar-capillary membrane is a unique structure which provides a large surface area for gas exchange yet also acts as a barrier against the indiscriminate leakage of fluid from capillary to alveolus. A number of adaptations exist which assist the membrane in its barrier functions. These include: (1) a pulmonary capillary pressure which is below the oncotic pressure of serum proteins; (2) an interstitial pressure which is subatmospheric; (3) a surfactant system which reduces intralveolar surface tension; and (4) an efficient lymphatic drainage system. However, the intrinsic structure of the alveolar-capillary membrane itself, does provide an effective barrier at the air-blood interface and any discussion of alveolar capillary membrane permeability must take this into account.

When lungs are fixed by vascular perfusion, electron micrographs show the alveolar-capillary membrane to be composed of the following structures going from alveolus to capillary(14) (Plate 1): surfactant layer, alveolar epithelium and its basal lamina, interstitium, the basal lamina of the capillary endothelium and finally the capillary endothelium itself. The alveolar septum is composed of a thick and a thin side, the difference being due to the amount of interstitium present. On the thick side the basal laminae are separated by portions of interstitial cells and scattered connective tissue fibrils. On the thin side the basal laminae are often fused

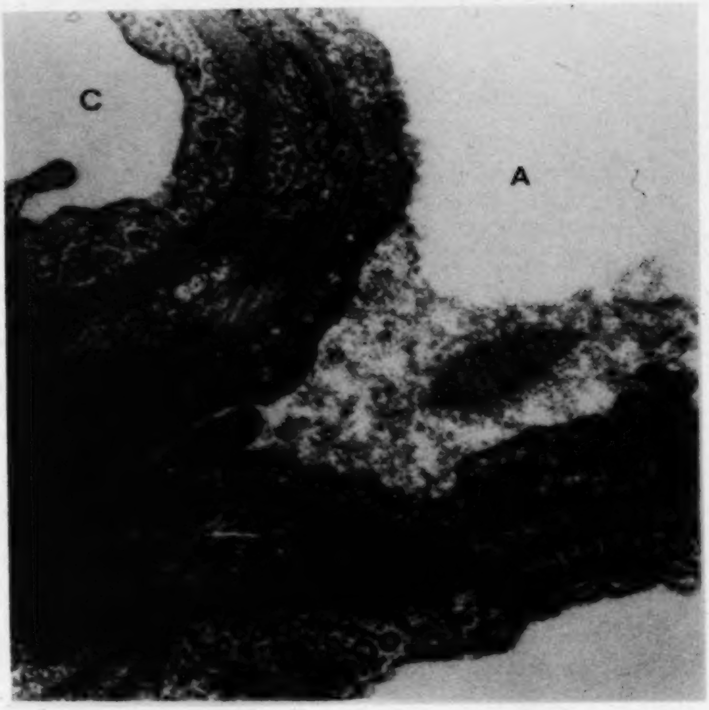

Plate 1 - An example of the alveolar-capillary membrane from an isolated perfused dog lung after perfusion-fixation. Surfactant is visible in the pleated "corner" of the alveolus (A), and layers of the alveolar-capillary membrane can be seen. The capillary (C) in the upper left lies on the thick side of the septum and the portion of the capillary in the lower right lies on the thin side. Reproduced with permission from Am. Rev. Respir. Dis.(14)

with very little intervening connective tissue. The thick and thin sides appear to be adapted for different functions; the thin side provides a thin barrier for gas exchange and the thick side provides a reservoir for excess interstitial fluid which appears to preferentially sequester on that side.(15) The thickness of the thick sides varies depending on lung size,(16,17) but that of the thin side appear to be similar in all mammalian lungs owing to the similar thicknesses of the alveolar epithelium and capillary endothelium. In the human lung, the air-blood barrier may be as little as 0.5 μm in thickness.(18)

The capillary endothelium is continuous and non-fenestrated and the cells contain numerous pinocytotic vesicles. These are the most conspicuous features of the cytoplasm and mitochondria, endoplasmic reticulum, and golgi complexes are only rarely seen.(19,20) The cell body containing the nucleus is usually found towards the thick side of the septum. The capillary endothelial cells are attached to each other by junctions in which a portion of the intercellular space is generally obliterated. However, some of these junctions have gaps approximately 4 nm in width which separate adjacent endothelial cells.(21) The presence of these gaps suggest that the capillary endothelium does not provide a totally impermeable seal between blood and alveolus. Indeed various workers have shown that these gaps known as tight junctions are the major sites of macromolecular translocation across the endothelium,(22) and that they can be widened by various disease processes.(23,24)

The alveolar epithelium is composed of a continuous layer of membranous, type I and granular, type II pneumocytes. Type I pneumocytes are characterized by broad cytoplasmic extensions (0.1-0.3 µm thick) which cover approximately 95% of the alveolar surface.(25) Type II pneumocytes, although slightly more numerous than type I pneumocytes, cover only the remaining 5%. The apparent paradox is due to the cuboidal nature of the type II cells compared to the flat, spread-out nature of the type I cells. The type I alveolar epithelial cells resemble the capillary endothelial cells in that they have numerous pinocytotic vesicles but are otherwise devoid of intracellular organelles. The type II cells, in contrast have numerous multivesicular bodies, multilamellar bodies(26) mitochondria peroxisomes(27,28) rough endoplasmic reticulum and a prominent golgi apparatus. Type II cells are responsible for pulmonary surfactant synthesis(29,30) and also serve as the progenitor of alveolar epithelial regeneration after pathological insult.(31) These functions are of special importance when considering the effects of radiation lung injury.

The alveolar epithelial cells, both type I and type II are joined to each other by tight junctions in a similar fashion to the endothelial cells. However, the tight junctions in the alveolar epithelium appear to be much tighter than those in the capillary endothelium, and of the 2 components of the alveolar-capillary membrane, the alveolar epithelium is the limiting structure in terms of molecular flux.(32-34) This was suggested in particular by the work of Taylor and Garr who, using the concept of reflection coefficients, showed that the pores in alveolar epithelium (most likely representing tight junctions) were about 0.8-1.0 nm in radius, and those in the capillary endothelium, 4.0-8.0 nm.(34) Various techniques have shown that clearance rates of solutes across the alveolar-capillary membrane are inversely related to molecular weight. Figure 1 shows that this inverse relationship is roughly maintained in a number of animal species regardless of the method of administration.(35) This hindrance of flux based on size criteria is compatible

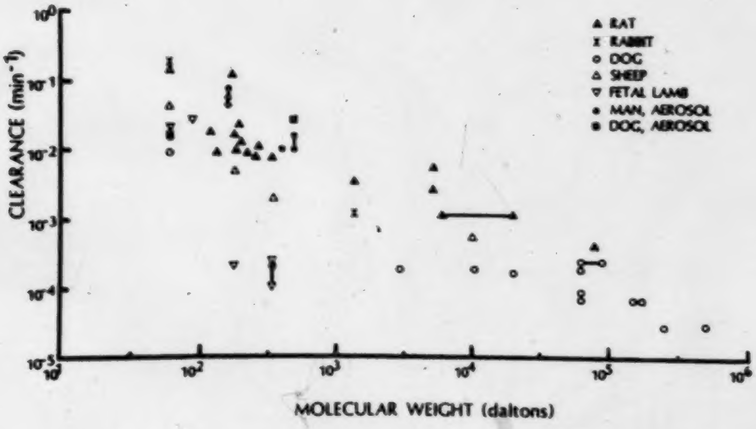

Figure 1 - Relationship between solute clearance from the lungs and molecular weight. Bars indicate range of molecular weights or clearance measurements. Clearances generally decline with increasing molecular weight and are higher in rats and following the administration of aerosols. Reproduced with permission from Am. Rev. Respir. Dis.(35)

with a diffusive mechanism. The work of Taylor and Garr suggests that, at least for the diffusive transfer of hydrophilic solutes, the alveolar epithelium is 5-8 times less permeable than the capillary endothelium.

Part of the difference in the permeability of the 2 layers may be due to the differing nature of the corresponding basal laminae: the epithelial basal lamina has a dense homogenous network of collagen fibres with fine 3-5 nm flaments running perpendicularly between basal lamina and the epithelial basal surface. Type IV and AB_2 collagen, heparan sulfate proteoglycans and associated glycoproteins (e.g. fibronectin and laminin) are the principal constituents of the epithelial basal lamina.(36) In contrast, the endothelial basal lamina contains a less dense and, more irregular array of heparan sulfate proteoglycans and as such displays only one fifth the number of anionic sites as the epithelial basal lamina.(36) In the glomerular basement membrane, heparan sulfate proteoglycans strongly influence basal lamina permeability(37) and if this is matched in the alveolar-capillary membrane, the proteoglycans may be partially responsible for this differential permeability.

The luminal surface of the alveolar epithelium is coated by the surfactant lining layer. On electron-micrographs this appears as a finely granular contour with a mean thickness of approximately 4 nm (Plate 1). The lining is made up of 2 parts - a surface film composed of highly surface active phospholipids (mainly dipalmitoyl lecithin) and a deeper hypophase layer containing phospholipid, carbohydrate and protein.(38-40) This surfactant layer, which may be missed, if the lung is not fixed in the appropriate manner(14), is of particular importance in radiation lung injury, and may also be important in alveolar-capillary membrane permeability changes in disease states.

Intercellular junctions

The intercellular junctions between alveolar epithelial and capillary endothelial cells have been the subject of much interest over the last 10-15 years. Until the early 1970's, it was firmly believed that the intercellular junctions - also known as tight junctions or zonula occludens, formed a complete seal between adjacent cells and that the transcellular route was the only way across the epithelium. This theory came tumbling down in 1972 when Frömter, on the basis of electrophysiological studies on the Necturus gall bladder, concluded that 90-95% of the passive ion flux across the tissue passed between cells.(41,42) Frömter and Diamond(41) were further able to classify various epithelia as either leaky (e.g. gall bladder, intestine, renal proximal tubule and choroid plexus) or tight (e.g. urinary bladder, stomach and frog skin) based on the degree of ion flux. Machen and co-workers(43) using ionic lanthanum as a tracer across the tight junctions were also able to classify epithelia as either leaky or tight depending on the degree of penetration of the tracer. In general there appeared to be a good correlation between the two classifications.(44)

When a tight junction is examined by transmission electron microscopy, the plasma membranes from adjacent cells appear to fuse at several points along the length. It has been possible, using a freeze fracturing technique to examine the inner aspects of the membranes, especially at the points of fusion.(45) Freeze fracturing of the junctions shows that at the points of membrane fusion, there are fibrils within the membranes. These fibrils form an irregular lace-like network(45) and seem to differ in various epithelia and also in different parts of the same epithelium or endothelium.(46)

The most frequently seen tight junction in the pulmonary capillary bed of mouse lung consists of 1-3 parallel, sometimes interconnected rows of particles present on a low ridge of the P face, and in a shallow groove on the E face. Because they are the most commonly seen type of junction, they have been tentatively identified as being in the capillary segment of the pulmonary vascular bed.(12) Simionescu et al have shown that there is a similarity in the appearance of the tight junction between various parts of the pulmonary vasculature and various parts of the mesenteric vasculature.(47) By comparison with mesenteric tight junctions, the different types of tight junction seen in the pulmonary vasculature have been tentatively identified as being either in the arteriolar or venular end. Of the three types of tight junction seen (capillary, arteriolar and venular), that of the arteriolar end appears to be the most complex and probably the tightest.

The tight junctions of the alveolar epithelium are much more complex and tighter than any seen in the pulmonary vasculature. They appear as a complex network of 3-6 smooth, continuous interconnecting fibrils on the P face and particle-free grooves on the E face. These appearances are similar to those seen in epithelia that are moderately impermeable to hydrophilic solutes.(48) Similar observations to those described above in mouse lung have also been made in freeze fractured dog lungs.(49)

Various investigators have attempted to correlate the "tightness" of the junction with its freeze-fractured appearance.(48,50) The correlation appears to be far from perfect(44) and this has lead to the suggestion that it may be the nature of the strands rather than the number which governs tightness. Van Deurs and Koehler for instance have suggested that it is the discontinuities in the fibrils that allow ions to navigate their way between the cells.(51)

Cytochemical techniques have, to date, failed to elucidate the chemical nature of the tight junctions. However, they appear to behave like fixed-charged gels with negative sites. This is of some importance in solute and especially ion translocation. For example in frog choroid plexus, these negative sites make the junctions more permeable to cations than to anions.(52) Olver and Strang have further shown that in fetal lamb lungs, cations traverse the epithelium more readily than do anions.(53)

Tight junctions, then, appear to be important in any discussion of alveolar-capillary membrane permeability. That they can be altered by chemicals, mechanical stress and disease processes(12,46) with a resulting change in solute permeability is especially relevant and will be discussed in a subsequent section.

Pathways for solute and fluid permeation

The permeability of the alveolar-capillary membrane is primarily dependent upon the lipid solubility of the translocating substance. Lipid soluble solutes and gases (possibly after dissolving in fluid lining the alveolus) translocate at a rate dependent on their lipid partition coefficients. This property is common to all epithelia and Figure 2 shows that this relationship holds for toad urinary bladder and a wide variety of substances of differing partition coefficients.(54) It should be noted, however, that small molecules have a higher permeability coefficient than can be explained by their partition coefficients. This is considered in more detail below.

Significant restriction to permeation across the alveolar-capillary membrane, therefore exists only for substances which are poorly lipid soluble. For these substances, 3 possible pathways across the alveolar-capillary membrane have been proposed. These are shown diagrammatically in Figure 3.(12)

The transcellular route, which clearly is the largest in terms of surface area is mainly for the passage of gases and lipid soluble substances mentioned above.(55) When permeability is related to molecular volume, there appears to be a steep inverse relationship between these 2 below 80 cc/mole. This has been taken as evidence for the presence of small aqueous pores approximately 0.45 nm in radius.(54) It has been suggested that these pores, may be

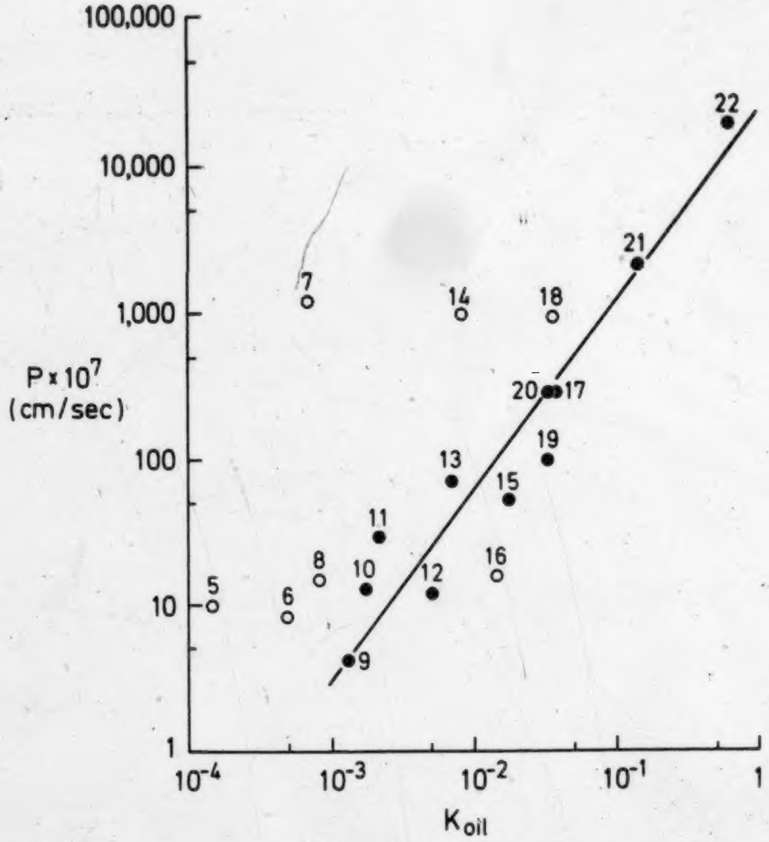

Figure 2 - Experimental relationship between permeability coefficients (P) and partition coefficients (K) for the toad urinary bladder. The line of identity was drawn to exclude small molecules (<60 cc/mole) which appear to have higher P's than predicted. The molecules are urea(5), ethylene glycol(6), water(7), acetamide(8), 1,3-propanediol(10), 1,4-butanediol(11), nicotinamide(12), 1,6-hexandediol(13), methanol(14), n-butyramide(15), iso-butyramide(16), 1,7-heptanediol(17), ethanol(18), antipyrine(19), caffeine(20), n-propanol(21) and butanol(22). Reproduced from Bindslev and Wright$^{(54)}$ with permission.

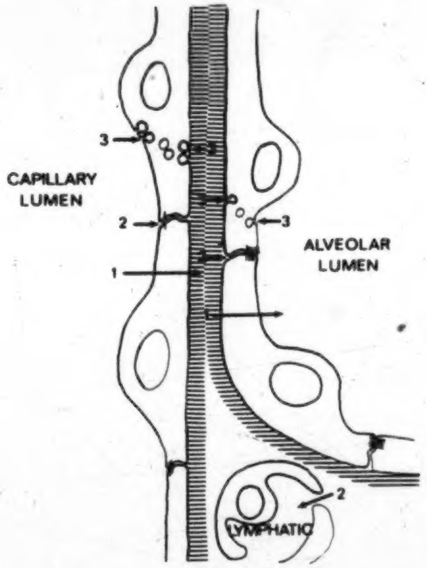

Figure 3 - A diagrammatic representation of the alveolar-capillary membrane. Pathways 1 and 2 represent the transcellular and intercellular routes, respectively. Pathway 3 represents the vesicular transport system operating across both epithelial and endothelial cells. Reproduced with permission from Fed. Proc.(12)

the sites of passive water (and possibly other small hydrophilic solutes) flux across the epithelium. Active transport mechanisms (considered below) probably also operate across the cells.

Although transcellular in nature, the pinocytotic route is considered a separate pathway by many workers. As mentioned in an earlier section pinocytotic vesicles are present in both the alveolar epithelial and capillary endothelial cells. They are probably the major pathway for protein and macromolecular flux across the alveolar-capillary membrane in health. The extent of this flux is controversial and will be considered below, but the consensus now appears to be that protein flux is small but finite. Schneeberger and co-workers documented the presence of horseradish peroxidase in epithelial pinocytotic vesicles after intratracheal instillation in newborn mice.(56) Similarly, following intravenous injection of horseradish peroxidase into adult mice, they showed the presence of the enzyme in endothelial vesicles.(21) Sapin and colleagues clearly showed that the pinocytotic vesicles of both type I pneumocytes and endothelial cells contain serum proteins(57) and that such proteins are present in the hypophase of the surfactant layer.(58) These findings support the concept of bidirectional vesicular transport of macromolecules across the alveolar-capillary membrane. However, the extent to which small hydrophilic solutes are carried by pinocytosis is not presently known.

The third pathway across the membrane is via the tight junctions. The structural features of the tight junctions have already been considered in some detail. Landis and Pappenheimer, in some classical studies(59) showed that nonfenestrated endothelia behave as though they contain water-filled pores 4 nm in radius. Michel, using the model of frog mesenteric capillaries, showed that these pores may be located in the tight junctions and that diffusion of ions and small hydrophilic molecules occurred in the area of the tight junctions.(60) Frömter also showed that in epithelia, the majority of ion flux occurred through the intercellular junctions.(42) As previously mentioned, Taylor and Garr demonstrated that pulmonary endothelium contains pores of 4-5.8 nm in radius, while those in alveolar epithelium measure only 0.6-1 nm.(34)

Various workers have shown that the intercellular junction and its permeability characteristics are susceptible to change following various manoeuvers.(46,61,62) So, although in health the junctions are the sites of ion and small hydrophilic solute flux, larger molecules may get across if the junctions are widened by intervention. In one experiment using horseradish peroxidase (molecular weight 40,000 daltons, molecular radius 3 nm), Schneeberger and Karnovsky demonstrated that if the enzyme was injected into mice in a large volume of saline, leakage occurred through the endothelial junctions, but was restricted in further passage by the alveolar tight junctions.(63) When the experiment was repeated with a small volume of saline the tracer remained confined to the capillary lumen.(64) These results were interpreted as indicating that a transient increase in intravascular pressure by the large volume of saline resulted in stretching of the endothelial tight junctions thereby permitting passage of tracer. The tightness of the alveolar lining compared to the endothelium was also confirmed. Pietra and colleagues, using isolated perfused dog lungs showed that at perfusion pressures of 15-20 mmHg, both horseradish peroxidase and hemoglobin remained confined to the lumen. Only when perfusion pressures were increased to 30 mm Hg and 50 mm Hg for horseradish peroxidase and hemoglobin respectively, did leakage of tracer occur.(65)

Finally, mention should be made of the "large pore theory" which has been developed to explain the greater flux of large polar solutes than can be explained by size criteria. Theodore and co-workers(66) examined the flux of several large molecular weight (60,000-90,000) solutes in an in vivo preparation of saline filled dog lungs. They found that the ratio of permeability coefficients of large polar solutes was similar to that of the ratio of free diffusion coefficients in aqueous solution. This similarity was used to argue that the diffusion in the tissue occurred through aqueous channels. Similar findings have been made in other epithelia.(67-69) It was concluded that the alveolar-capillary membrane contained several large pores (pore-radii > 32A°) through which these solutes could pass.(66) The anatomic location of these pores has not been clearly established, and the possibility still exists that this transport may occur by pinocytosis. Moreover, the saline-filled dog lung clearly does not equate with normal physiology; alterations in the permeability characteristics may have resulted from the effect of saline on alveolar tissue or by stretching of tight junctions by the increase in intra-alveolar pressure.

The translocation of water across various epithelia has been measured in a way similar to other substances. Clearly, hydrostatic and osmotic gradients will alter the degree of flux, but in the absence of these forces, values for permeability in the range of 1 X 10^{-6} to 1 X 10^{-2} cm/s have been obtained.(70) In toad urinary bladder and rabbit gall bladder, the transepithelial permeabilities are 1 - 2 X 10^{-4} cm/s.(71) These values are compatible with a transcellular route for water flux. As mentioned above, osmotic and hydrostatic pressure gradient can also lead to water flux, and of the 2, hydrostatic pressure appears to be more effective. Diamond(72) working on toad gall bladder has clearly shown that active sodium transport provides the driving force for water absorption. Transport of sodium from mucosa to serosa occurs in 2 stages: (1) entry into the epithelium from mucosa down the electrochemical gradient across the apical membrane and (2) subsequent transport out into the lateral intercellular spaces by Na^+ pumps in the basolateral membrane. The scheme described above is common to epithelia in general(73,74) and therefore probably also applies to the alveolar epithelium.

Mention should be made of the pathways for fluid flux across the barrier in pulmonary edema. In nonhemodynamic pulmonary edema, flux is probably direct via the damaged alveolar-capillary barrier. In hemodynamic pulmonary edema no such damage exists(15) and there is still considerable speculation about the pathways involved. Nelson and co-workers(75) found that in high pressure pulmonary edema, although there was free flow of plasma protein tracer into the air spaces, there was no free flow of alveolar protein tracer in the opposite direction. Zumsteg et al(76) confirmed that liquid enters directly from the alveolar wall via the microvascular interstitium in increased permeability edema. In high pressure edema, on the other hand, they could not locate the site of the pathway for alveolar flooding, although it was not directly through the alveolar epithelium. To explain these obervations, Gee and Staub proposed that alveolar flooding occurred in an all or none fashion via so-called high conductance pathways.(77) They suggested that as the excess fluid accumulates in peribronchovascular cuffs, the pressure gradually rises. Eventually, a situation is reached when interstitial pressure is greater than alveolar pressure and fluid leaks into the alveoli through discrete breaks. They have proposed that these breaks may occur at the bronchiolar-alveolar junctions but no direct evidence exists. Indeed the regional permeability characteristics of the air-blood barrier, are at present unknown. Yoneda(78) has examined the intercellular junctions in the upper, mid and lower zones of the human lung and found that no differences exist in the alveolar epithelium. In the capillary endothelium, however, the number of strands in the tight junctions increased from the upper zone (2.80) to the lower zone (4.99).

Throughout the discussion of solute flux across the alveolar-capillary membrane, it has been assumed that translocation is by passive means. However this may be an erroneous assumption and studies on flux must take into account the possibility of active transport. Active chloride secretion in canine tracheal epithelium(79) and bullfrog lung(80) have been well described and investigated. Recently, active transport of phenol red(81) and disodium cromoglycate(82) have been described in lung. We have also recently shown that sodium pertechnetate which has been used to assess the barrier properties of the alveolar capillary membrane (see later), acts as a pseudohalide and is transported from serosa to mucosa by active means.(83)

Methods of measuring alveolar-capillary membrane permeability

Various techniques have been employed to assess the permeability characteristics of the alveolar-capillary membrane. One of the earliest and possibly most ingenious was that of Chinard who used the multiple indicator dilution technique.(84) The principle of this method was that multiple indicators could be injected into the pulmonary circulation and the disappearance of a test indicator could be compared to an indicator known to be impermeant by means of several blood samples. Taking into account initial quantities of injectate, extraction ratios could be obtained. Typical curves are shown in Fig.4.

These initial studies measured mainly endothelial permeability and although ingenious had several limitations. In vivo studies were limited to first pass measurements because of the unknown volumes of distribution of the test indicators. Although corrections could be made, these required the labeling of the whole circulation which proved to be expensive. For substances which had low permeabilities, much longer time periods were required and these, of course, lead to further problems related to volume of distribution and excretion. Chinard later used this technique to assess movement of substances from alveolus to capillary.(32) In this method indicators were placed in a small volume of fluid in the lung and flux was assessed by measuring the rising concentrations of the substances in the

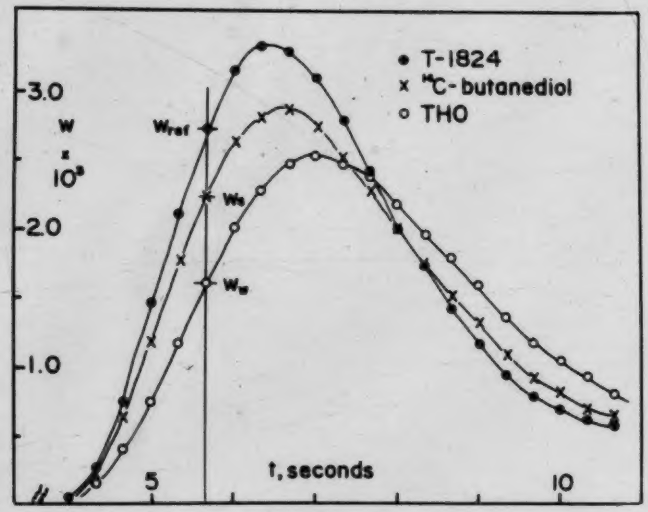

Figure 4 - Typical curves obtained from a multiple indicator-dilution experiment in which ^{14}C-butanediol is the test substance and T-1824 the vascular (impermeant) tracer. THO is a reference tracer with some flow-limited distribution. The ordinates, W, indicate the concentration of the substance in the outflowing blood divided by the amount injected. The abscissas, t, indicate the time after injection. The position of the curve for butanediol intermediate to the two reference curves is evidence of extraction of the substance from the blood into tissue. Reproduced with permission from Microvasc. Res. (84).

pulmonary circulation. Again similar problems were present. He concluded however that the alveolar-capillary barrier was very permeable to water, dissolved carbon dioxide and gases such as tritium, ethylene, krypton and xenon. However, there appeared to be marked restriction to the passage of sodium and bicarbonate ions and urea.

The problems related to in-vivo studies were largely overcome by in-vitro lung preparations. Using this technique in dogs, Taylor, Guyton and Bishop(85) showed that the alveolar membrane behaved like other cell memebranes in that it was permeable to water and DNP, a fat-soluble substance, but much less permeable to Na^{24}, K^{42} and urea. They concluded that the alveolar epithelium was the limiting barrier of the alveolar-capillary membrane. Wangensteen et al using a rabbit lung preparation,(86) came to similar conclusions. They assessed both the overall barrier by measuring perfusate levels of indicator after alveolar instillation and the endothelial barrier by measuring disappearance rates of indicator from perfusate.

More recently, these techniques have been slightly modified for use in-vivo. Egan(87) has used a popular model in which a segment of lung is isolated by a catheter wedged in the bronchus. The air space distal to the catheter is collapsed and then filled with a normal saline solution containing several radiolabeled hydrophilic solutes of known molecular sizes. An impermeant solute (e.g. albumin or inulin) is also included in the cocktail. Measurement of the concentration of the solutes in alveolar liquid over time provides a relationship as shown in Fig.5. The impermeant solutes have parallel slopes and increasing concentrations because of the absorption of water. The rates of loss for the permeant solutes (sucrose, mannitol and urea) are calculated by subtracting the slopes of these tracers from those of the impermeant tracers.

Theodore and co-workers(66) looking at the flux of large polar solutes used the opposite approach. They instilled saline into a degassed portion of the left lower lobe and following an intravenous injection of sucrose, inulin and dextran measured increasing concentrations of these substances in alveolar fluid. They basically concluded that flux of these substances in the saline-filled dog lung model was significant and proposed that large pores must exist in the alveolar epithelium, to account for this. Their method was limited however by the need to label the whole circulation.

An alternative though much more indirect approach to assess endothelial flux is to measure lymph flow rates in a chronic animal preparation.(88-90) These methods have been principally used to look at fluid flux and Staub has been the main proponent of this technique. He used a chronic sheep preparation in which the efferent duct of the caudal mediastinal lymph node was cannulated and the tail of that node resected to eliminate lymph not originating in the lungs. Using this preparation, Brigham and associates(91)

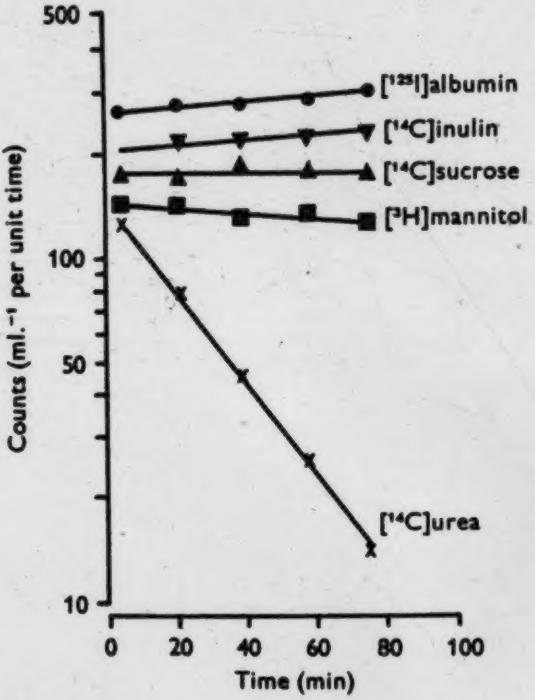

Figure 5 - Relationship of the change in concentration of solutes in alveolar saline with time. Regression lines calculated by least squares. Reproduced with permission from Am. Rev. Respir. Dis.(87).

have studied the sieving characteristics of the endothelial barrier by infusing dextrans of different sizes into sheep and observing their partitioning between blood and thoracic duct lymph. Wasserman, Mayes and Loeb(92) did a similar study in dogs. They found that the permeability of the endothelium is related to molecular weight of tracer and that interestingly the endothelium of dog is less permeable than that of sheep.

Many of the techniques thus far mentioned have limited applications in clinical medicine. Although useful in documenting the overall permeability characteristics of the membranes to specific substances they were invasive and too cumbersome to be used in clinical situations. Moreover measurements of airway concentrations could be misleading if the instilled solution became diluted by fluid already in the airspaces. These solute concentrations could also be influenced by subsequent fluid accumulation and reabsorption within the lungs. What was required was a simple technique usable in humans which would easily tell whether the membrane had become abnormally permeable or not. Hemodynamic and non-hemodynamic pulmonary edema are two good examples in which data on the permeability characteristics would be important.

Jones and co-workers(93) in some preliminary experiments, instilled a cocktail containing ^{51}Cr EDTA and ^{125}I-antipyrine into rabbit lungs. ^{51}Cr EDTA is a small hydrophilic solute with a molecular weight (MW) of 377; ^{125}I-antipyrine is highly lipid soluble and has an M.W. of 312; both are γ emitters. The relative extractions of the 2 substances were recorded by measuring the radioactivity in serial blood samples. The ratio of the specific activities of the tracers in the cocktail was used to convert the activity of tracers in blood so that they could be compared directly. In animals with normal lungs, the 2 tracers showed a characteristic pattern - illustrated by Fig.6(a).

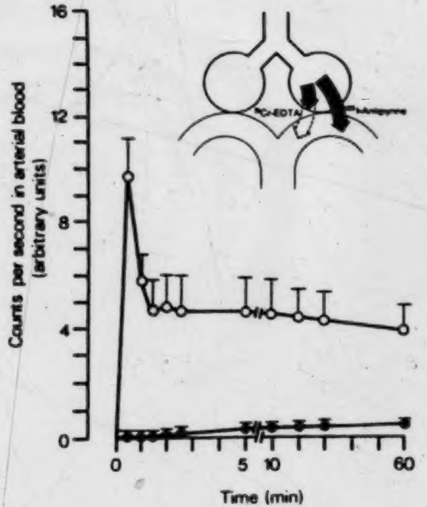

Figure 6a

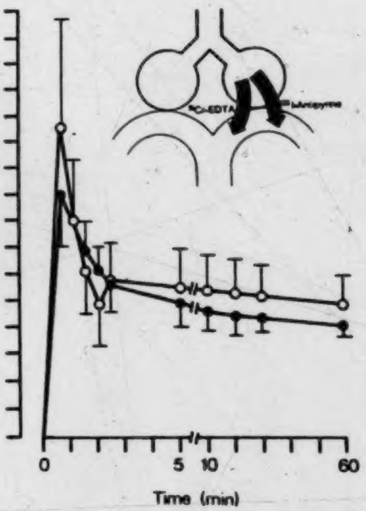

Figure 6b

Figure 6a and 6b - Sequential arterial blood samples analyzed for ^{51}CrEDTA (●) and ^{125}I antipyrine (○) immediately after injecting a bolus of the two tracers into the airway. Figure 6(a) illustrates the result in normal lungs. Figure 6(b) shows the result after the instillation of HCl (2 ml/kg; pH,1) into the airways prior to the bolus injection.

Reproduced with permission from Br. J. Anesth.(93)

The blood level of ^{125}I-antipyrine peaked 15 to 30 s after injection and then showed a fall to a gently decaying plateau. The ^{51}Cr EDTA appeared slowly in very low concentrations. An index of permeability was expressed as the ratio of the area under the ^{51}Cr EDTA curve to that under the ^{125}I-antipyrine curve during the first 5 min after bolus injection. In normal animals, the ratio ^{51}Cr EDTA/ ^{125}I-antipyrine was 0.02.(93)

Jones et al produced alveolar epithelial damage by instilling hydrochloric acid into the lungs (10^{-1} M) and showed that the index increased to unity with the activity/time curves for the 2 tracers virtually superimposed.(93) This is shown graphically in Fig.6(b). They further showed that both intravenous adrenaline(94) and exposure to carbon monoxide(95) increased permeability and this was accompanied by electron microscopic changes.

Although much less cumbersome than earlier methods, these techniques were still invasive. Damage to the alveolar and airway membranes during instillation and subsequent sampling was a distinct possibility.

Many of these problems were largely overcome in the late 1970's with the introduction of the tracers into the lungs by means of an aerosol. Aerosols were found to be more readily administered in a clinical setting and were less likely to lead to injury, atelectasis, infection or impaired gas exchange. Chopra and colleagues at UCLA(96) were one of the first proponents of this technique. The principle of the technique was to aerosolize solutions of radiolabeled solutes into the lungs. Provided the aerosol particles were small enough to reach the alveoli, the clearance rates from the lungs as monitored by a suitable external detector could be used as an index of alveolar-capillary membrane permeability. Most workers used aerosols of ^{99m}Tc-diethylenetriaminepenta-acetate (DTPA, MW 492) and sodium pertechnetate (TcO_4^-, MW 163). Aerosol particles in the size range 1-2 μ were produced usually by passing the aerosol through a reservoir bag interposed between the nebuliser and the mouth piece.(96,97) This allowed particles larger than 2 μ to settle out in the bag by sedimentation. Various workers have shown that the optimal range of particles for alveolar deposition is 0.3-2 μm,(98) and as such particle sizes used in these studies were probably appropriate for alveolar deposition. The deposition sites were therefore distal to the mucociliary escalator and clearance rates could be used as an index of alveolar-capillary membrane permeability. One of the major problems with this technique was how to separate activity present in the alveoli and terminal airways during washout from activity in the chest wall. Jones and co-workers(99) monitored activity both over the lungs and over the thigh. During washout, when activity had fallen to approximately 50% of the initial activity, they injected an intravenous bolus of ^{99m}Tc DTPA. From the relative increases in activity in the 2 fields, a correction factor was derived and was used to subtract the appropriate fraction of the leg tracer activity from the lung activity. In this way they obtained a clearance curve for lung activity alone.

This technique for measuring alveolar-capillary membrane permeability has been used by many investigators. It is largely non-invasive and simple, and by the use of mobile detection systems it can be adapted to look at patients in the clinical setting. The clearance rates obtained for normal subjects seem to be fairly reproducible in the hands of individual workers, but as expected there are species differences.(100) Table 1 summarizes some of these results.

The importance of this technique is that it is able to pick up abnormalities in permeability which may have important therapeutic considerations. Permeability changes in various lung conditions have been documented using this technique and these will be discussed in the following section.

It is important to note that in most of the methods for measuring alveolar-capillary membrane permeability so far mentioned, measurements probably reflect both alveolar-capillary as well as terminal bronchiolar capillary membrane permeability. Differentiating between the 2 is very difficult but it is likely that the alveolar component is dominant in view of its greater surface area. Strictly speaking, therefore, a better term would be pulmonary permeability - this being a combination of the alveolar and bronchiolar components. In the text that follows therefore, the term pulmonary permeability is used instead of alveolar-capillary membrane permeability.

Table I

SPECIES DIFFERENCES IN HALF TIME CLEARANCE FROM LUNG TO BLOOD (T ½ LB)

Species	T ½ LB (min)
Rabbit (101)	260
Rat (102)	
Female	114
Male	44
Man (99)	59
Dog (103)	25

Half-time clearances of isotope from lung to blood (T ½ LB) in various animal species showing inter-species variation.

Alterations in pulmonary permeability

In 1975, Egan and co-workers(104) showed that pulmonary permeability was not static and could be altered physiologically. Studying fetal lambs at the onset of breathing and over the next few hours, they noticed that as fetal lung liquid was absorbed, the equivalent pore radii of the epithelium increased to an average of 4.0 nm. When lambs were studied several hours after birth, when most of the fluid had been absorbed, the pore radii had reduced to 1.1 nm. It appeared that the increase in the size of pores, at the onset of breathing facilitated the absorption of protein. Egan went on to show, however, that the alteration in permeability was probably more related to an increase inflation volume rather than anything else.

Over the last 8 years a number of publications have appeared, primarily from Egan et al(105-107) who have further characterized changes in pulmonary permeability following lung inflation. They studied pulmonary permeability to solutes at different levels of lung inflation in adult sheep.(105) Their results are presented in Fig.7 and show that as inflation volume increases, equivalent pore radii also increase. At the extremes of lung inflation (termed leaks) all barrier properties are lost and solutes of all sizes (including proteins) pass through into the alveoli. Total lung volume in these experiments was defined as the volume of gas the

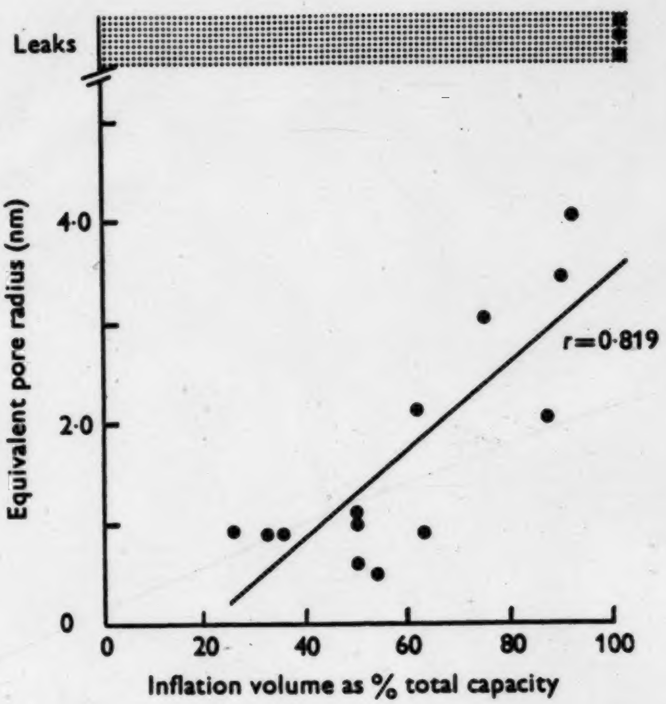

Figure 7 - Relationship between lung inflation and calculated alveolar epithelial pore radius in adult sheep in vivo. Reproduced with permission from J. Physiol. (London)(105)

experimental section of the lung could contain at 40 cm of water pressure. Lung inflations were usually maintained for approximately 10 min in each study. Similar results were obtained in dogs(106) in whom the effects of 3 low volume inflations (47% of total lung capacity) were compared to 3 high volume inflations (82% of total lung capacity). Their results are shown in Fig.8. When low volume inflations were followed by high volume inflations the pore radii universally increased. When high volume inflations were

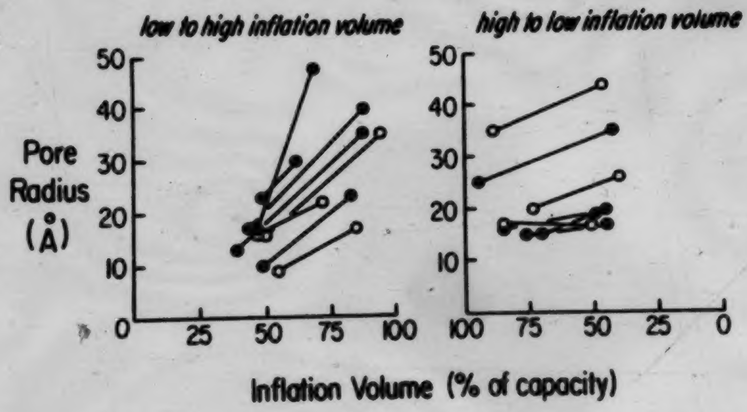

Figure 8 - Relationship between inflation volume and alveolar epithelial pore radius in consecutive inflations in adult dogs. Open circles represent animals that appear on both panels. Reproduced with permission from J. Appl. Physiol.(106)

followed by low volume inflations, the pore radii did not immediately decrease, and either stayed the same or actually increased. These results were interpreted as showing that high volume lung inflations produced epithelial injury rather than deformation and more than just the release of inflation was required for a return to normal pore radii. Egan(107) has also recently shown in rabbits that if the whole lung is inflated in situ for 20 min with 40 cm of water pressure, its resting volume increases by 350% but there is no change in protein permeability of the membrane. If only an isolated segment is hyperinflated, the segment increases its volume between 5 and 10 times by displacing other structures in the thoracic cavity. With this degree of distension the epithelium becomes permeable to proteins.

Kim and Crandall(108) working on bullfrog lungs had similar results. They found that when the lungs were inflated to 50 cc, equivalent pore radii did not change significantly from those at 5 cc inflations. When the lungs were hyperinflated (>80 cc) the pore radii increased to 3.4 nm (from 1.1 at 5 cc). They concluded that the alveolar-capillary membrane retains its barrier properties in the range of lung volumes encountered in vivo; however at lung inflation higher than this, barrier properties are compromised. The clinical correlate is that in patients with lung disease in whom parts of the lung have different compliance characteristics, hyperinflation of high compliance segments (especially if artificially ventilated) may occur leading to possible alteration in pulmonary permeability.

Besides the changes in pulmonary permeability mentioned above, changes also occur in various disease states. Possibly the most important of these is pulmonary edema. It has long been recognised that there are 2 major types of pulmonary edema; hemodynamic pulmonary edema in which the Starling forces are altered allowing alveolar flooding, and nonhemodynamic pulmonary edema in which damage to the alveolar-capillary membrane allows the inward flux of edema fluid. Mason and colleagues(109) have shown that alveolar clearance rates of aerosolized DTPA are much faster in patients with nonhemodynamic than hemodynamic pulmonary edema. Anderson et al,(110) measuring the alveolar flux of intravenously injected ^{131}I-labeled human serum albumn by alveolar lavage found that clearance rates of the radionuclide were much greater in patients with Adult respiratory distress syndrome (ARDS) than in patients with hemodynamic pulmonary edema. Both these studies confirm that non-hemodynamic pulmonary edema is an alveolar capillary leak condition and that differentiation from hemodynamic pulmonary edema is possible using these techniques.

Rinderknecht et al(97) have shown that in various types of interstitial lung disease, (5 with idopathic pulmonary fibrosis, 4 of 8 with sarcoid, 2 of 5 with pneumoconiosis) clearance rates of DTPA and TcO_4^- are increased. In pulmonary alveolar proteinosis(97) clearance rates of TcO_4^- are decreased, but return towards normal after alveolar lavage. In COPD clearance rates of DTPA were unchanged. Chopra and colleagues(96) showed that the clearance rates of DTPA from the lower lung zones were considerably faster in patients with systemic sclerosis than normals. Both the previous studies showed that in normals, examined in the erect position, clearance rates of solutes were faster in the upper than lower zones. Rinderknecht et al(97) further showed that this differential clearance for TcO_4 could be removed by breathing against 7 cm of H_2O positive end expiratory pressure. They concluded that the clearance of the solutes was probably not related to perfusion (which is greatest at the bases) but possibly surface area for diffusion. At functional residual capacity in the erect position alveoli in the apices are larger than in the bases but this difference is removed if the lung is inflated to total lung capacity. They postulated that the increased clearance of solutes in these diseases was possibly related to increased retractive forces.

In asthmatics, O'Bryne et al(111) found an increased clearance of DTPA compared to normals; after histamine challenge, the increase in permeability in asthmatics was greater than the increase in normals. This alteration in pulmonary permeability seen in asthma is not accepted by all workers however and has recently been re-examined by Elwood et al(112) who found no difference in stable chronic asthmatics compared to normals.

Apart from physiological alterations in pulmonary permeability and those seen in disease, permeability characteristics can be altered by intervention.
Some mention has already been made regarding this in the studies by Jones et al(93) who found that ^{51}Cr EDTA flux increased after alveolar instillation of acid. Most of the permeability changes induced by intervention have focused on the effects of cigarette smoking. There has been considerable recent interest in these effects and generally the results of various workers are in agreement. In summary, it appears that cigarette smoking increases the

alveolar clearance of DTPA.(93) In animals this has been shown to be a rapidly induced effect(113) (100 puffs of cigarette smoke) with recovery within 12 hours of cessation. In humans this increased permeability reverts to normal after about 7 days.(114) That this increased flux of DTPA is due to a widening of the intercellular junctions has been shown by cytochemical techniques in which horseradish peroxidase (MW 40,000 daltons) was seen to penetrate the tight junctions in guinea pigs exposed to cigarette smoke.(113,115) In trying to determine what factor of cigarette smoke increases permeability, Jones et al(116) have shown a hyperbolic relationship between carboxyhemoglobin concentrations and DTPA T $\frac{1}{2}$. Minty and co-workers(117) have demonstrated that nicotine is probably not an important factor and have argued(114) that although the change in permeability may be due to a direct effect of the constituents of smoke, alveolar macrophages which are increased in smokers may play a part.

Radiation lung injury

The deleterious effects of radiation on the lung have been recognised for many years. The first reports originated in 1922 from Groover, Christie and Merritt.(1) These were followed by many others(118,119) and it quickly became appreciated that lung injury was the limiting factor in radiotherapy treatments to the lung, mediastinum and chest wall. Two fairly well defined syndromes have been described: radiation pneumonitis, which is an exudative reaction of the lung occuring 3-6 months following the start of irradiation and radiation fibrosis which is a late reaction occuring months or years later. The incidence of these 2 syndromes, especially pneumonitis, has been difficult to determine because of the differing radiation schedules employed and doses used. Nevertheless it is accepted that radiation fibrosis probably occurs to some extent in all patients given radiation therapy. In most instances it is asymptomatic. In contrast, radiation pneumonitis probably occurs in a minority (5-15% of all patients irradiated)(2) yet accounts for most of the morbidity and mortality seen in radiation lung injury. The clinical and physiological features of these syndromes have been well described.(2,13,120)

Regardless of the dose of radiation used there appears to be a latent interval between radiation exposure and the onset of symptoms or physiological and radiological abnormalities. In trying to elucidate the pathogenesis of radiation lung injury most workers have concentrated on this time frame under the assumption that damage occurs at the time of irradiation but that its manifestation is delayed. It has been well established that histological changes occur before clinical and radiological abnormalities(13) and indeed some workers have shown ultrastructural changes within 24 hours of irradiation(5) For the purpose of this review, consideration will be given to the morphological changes seen in radiation lung injury as these best describe the changes in alveolar-capillary membrane permeability that may arise.

Warren and Spencer(6) were probably the first investigators to describe the histological features of radiation pneumonitis: (1) swelling and distortion of the alveolar lining cells with some desquamation, (2) formation of a characteristic but inconsistant hyaline membrane usually closely adherent to the alveolar wall associated with congestion and edema, (3) progressive fibrosis with hyalinization of arterial and alveolar walls and (4) a mild, nonspecific inflammatory response. They considered the combination of hyaline membranes and alveolar anaplasia almost pathognemonic of radiation pneumonitis. Since that time, particularly with the introduction of the electron microscope, numerous workers have tried to further characterise these changes. Because of the lack of suitable human tissue most workers have concentrated on animal studies and have looked at the effects of both single and multiple fractionated doses of radiation.

Table 2 summarizes the changes seen in different parts of the lung for the immediate and early (0-2 months) intermediate (2-9 months) and late (9+ month) stages of radiation lung injury.(13) What the table hides however, is the great variability in the effects on alveolar epithelium and capillary endothelium. Phillips(5) has shown that after 20 Gy to the thorax in mice, endothelial changes occur as early as 24 hours. These consist mainly of segmental separation of the endothelium from the basement membrane and scattered vacuoles or blebs within the endothelium. At 2 months, the changes are much worse with endothelial sloughing and apparent obstruction of capillary spaces by separated endothelium. The most surprising finding of Phillips' study was the minimal change in alveolar epithelium. Mousavi and co-workers(7) similarly found that the endothelial cells were the first to be damaged after 35 Gy to the lung of dogs. Their changes occurred at 14 days post-exposure with capillary dilatation, congestion and increased pinocytosis. They did, however, document alveolar epithelial changes at 14-28 days post-exposure. These consisted mainly of thickening of the alveolar septum with edema fluid and patchy fibrosis.

In contrast to the above studies, Leroy and co-workers,(8) Faulkner and Connolly,(9) Penney and Rubin(10) and Travis(11) have all found that the initial and most severe damage occurs to the alveolar epithelium and

Table 2(a)

MORPHOLOGICAL LUNG CHANGES AFTER THORACIC IRRADIATION

Immediate and Early (0-2 months)	Intermediate (2-9 months)	Late (9 months+)
2 Hours		
Endothelial cell changes (121)	Marked capillary abnormalities widespread obstruction due to platelet, fibrin and collagen (5,121-123)	Loss of many capillaries, regeneration of new capillaries (122,124)
2-7 days		
Progressive, marked endothelial cell changes with separation from basement membrane (121,123,125,126) and sloughing (127) leading to luminal obstruction	Regeneration of capillaries (123)	

Table 2(b)

MORPHOLOGICAL LUNG CHANGES AFTER THORACIC IRRADIATION

Immediate and Early (0-2 months)	Intermediate (2-9 months)	Late (9 months+)
Type 1 Pneumocytes		
Degenerative changes (121,123, 125,126) or normal (128)	Decreased number (121)	Further decrease in number (121)
Type 2 Pneumocytes		
Very early degenerative changes (121) becoming more marked with time (8,121,125) normal (123)	Large increase in size and number, with abnormal appearance (121,122)	Return to normal size and number (121,122)
Basement Membrane		
Early swelling, indistinct (8,121, 125,128) later very irregular (125)	Folded and thickened (122)	Folded and thickened (122)

Table 2(c)

MORPHOLOGICAL LUNG CHANGES AFTER THORACIC IRRADIATION

Immediate and Early (0-2 months)	Intermediate (2-9 months)	Late (9 months+)
Interstitial Space		
Edema and debris (121,125-127), infiltrated with inflammatory cells (128) and basophils (126). Slight increase in connective tissue (128)	Infiltrated with mononuclear cells (124), mast cells (124, 126) inflammatory cells (122) and connective tissue (121-123, 124,126,127)	Few inflammatory cells (122,124) large increase in collagen(5, 121,122,124)
Alveolar Space		
Fibrin, hemorrhage and debris (121, 128) increased number of alveolar macrophages (125,126)	Becomes smaller (124)	Small or absent, distortion of architecture (5,121,124)
Bronchial Epithelium		
Early transient inflammatory reaction, ciliary paralysis, increase in goblet cells (129) or normal (123)	Epithelial proliferation (129)	

in particular to the type II or granular pneumocytes. These latter workers were in general agreement as to the changes seen. For example, Penney and Rubin(10) found that with light microscopy the early changes were restricted to alveolar and septal edema. At the ultrastructural level, in addition there was fibrin deposition, histocytic invasion and fibrosis. The most pronounced alteration was the marked depletion in the number of lamellated bodies in type II pneumocytes. Lamellar body depletion was usually followed 7 days later by cellular hypertrophy and increased numbers of lamellated structures. Following longer post-irradiation periods some type II cells exhibited characteristics of cell degeneration (vacuolation, mitochondral swelling, distension of the endoplasmic reticulum) and finally were sloughed into the alveolar lumen. Changes in the capillary endothelium were often seen, but in general were mild. These differences in findings are difficult to explain but are probably not due to species differences or to the dosage of radiation used.

Regardless of which cell is primarily affected it is fairly clear that both the capillary endothelial and alveolar epithelial (especially the type II pneumocyte) cells are damaged at some stage following radiation exposure. The most consistent findings in all the studies so far cited is the thickening of the alveolar septum with edema fluid and fibrosis. Penney and Rubin(10) postulate that this thickening of the alveolar-capillary membrane is likely to impair oxygen transfer. Although they found severe damage to the alveolar epithelial lining they state that "no morphological breaks or denudation of alveolar wall were observed at any of the dosages employed".

From the above considerations it is clear that the major components of the alveolar-capillary membrane are damaged in radiation lung injury. A change in alveolar capillary membrane permeability is therefore a strong possibility. In view of this change occurring in the latent period, it is quite possible that an alteration in permeability may be an important step in the pathogenesis of radiation lung injury. If so, documentation of this change would be useful. An index of permeability could then be used in studies on prevention and treatment and if the test employed was adequately non-invasive, it could be used also in the clinical setting.

CHAPTER III

EXPERIMENTAL

Summary of protocol

(A) Animal selection

(B) Pre-irradiation radioaerosol scanning

  (i) Isotope preparation and quality control

  (ii) Aerosol generation

  (iii) Radioaerosol scanning

  (iv) Blood background determination

(C) Conventional pre-irradiation imaging

  (i) Chest radiography

  (ii) MAA perfusion scanning

  (iii) CT scanning

(D) Irradiation

(E) Post-irradiation imaging

(F) Measurement of lobar compliance

(G) Morphology

(A) Animal selection

Twelve short-haired mongrel dogs with normal anterior-posterior chest roentgenograms were used in this study. Their weights prior to irradiation ranged from 16.7 to 26.1 kg [mean 21.35 ± 2.54 (SD)].

(B) Pre-irradiation radioaerosol scanning

(i) Isotope preparation and quality control

DTPA was freshly prepared prior to each scan by adding TcO_4^- (815 MBq in 2 mls of normal saline) to DTPA kits (Frosst, Montreal, Canada). The stability of the ^{99m}Technetium-DTPA complex was assessed by means of thin layer chromatography (Gelman IT LC-SG). Analysis of the strips was performed on a Canberra series 40 multichannel analyzer (Canberra Industries Inc., Meriden, Connecticut) connected to a Berthold model LB 2832 automatic TLC linear analyser (Berthold, Wildbad, W. Germany). The stability checks were performed on random days at the beginning of the study on samples taken from the nebuliser both before and after nebulization. In addition, chromatography was performed on DTPA aerosol particles trapped by a paper filter at the exit port. All analyses showed that at least 96% of the pertechnetate was bound to DTPA.

Sodium pertechnetate was obtained from the Edmonton Radio-pharmaceutical Centre.

(ii) Aerosol generation

The experimental set-up was as shown diagrammatically in Figure 9. Aerosols were generated from 2 cc of the solution (600 MBq of TcO_4^- or 815 MBq of ^{99m}Tc-DTPA) placed in a DeVilbiss #40 nebulizer operating at 30 psi air pressure. An 8 litre rubber bag enclosed in a lead-lined lucite box was interposed between nebulizer and dog to remove large particles (>2 μm) by sedimentation. The resulting particles as measured by an 8-stage cascade impactor (Andersen Samplers Inc., Atlanta, GA) were found to have an activity median aerodynamic diameter (AMAD) of 1.2 μm and geometric standard deviation (σg) of 1.8 μm.

(iii) Radioaerosol scanning

The dogs were anesthetised with intravenous pentobarbital (Barbital)(30 mg/kg), intramucular acepromazine maleate (Atravet)(1 mg/kg) and intubated. A solution containing 3.3% glucose and 0.3% saline (50 cc's/hour) was given intravenously and additional doses of pentobarbital administered as necessary to maintain anesthesia. The dogs were positioned supine with the anterior chest wall in close opposition to the face of a gamma camera. On experimental days the TcO_4^- scan always preceded that of DTPA in order to have the least background counts for the fastest clearing isotope. Prior to inhalation, the dogs were given 5-7 hyperinflations for one minute (15-20 cc/kg) to minimize areas of atelectasis and to

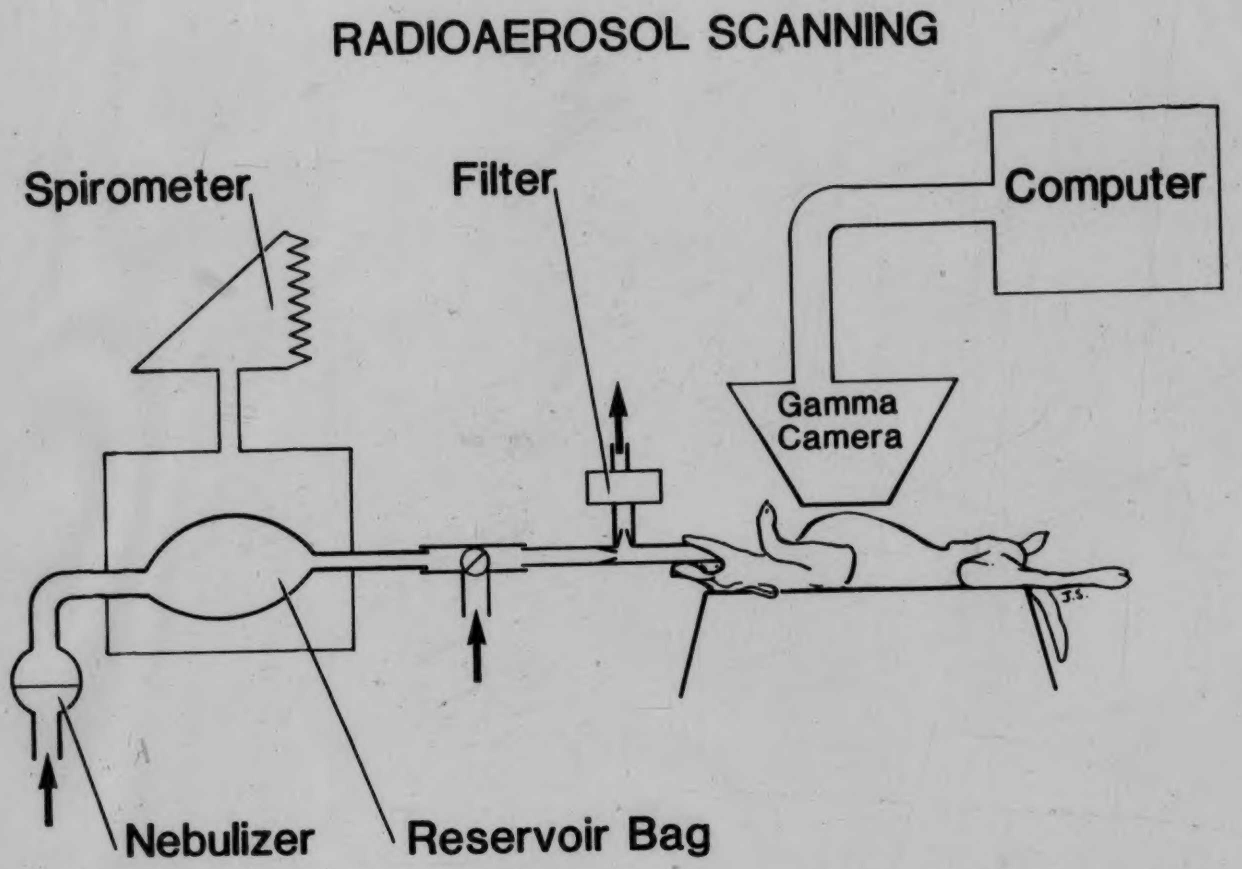
RADIOAEROSOL SCANNING
Spirometer
Filter
Computer
Gamma Camera
J.S.
Nebulizer
Reservoir Bag

Figure 9 - The experimental circuit showing a dog positioned under the gamma camera and the aerosol generation system of nebulizer and reservoir bag. A spirometer measured inspiratory excursions and expired particles were trapped in the filter shown.

aid aerosol penetration. The dogs inhaled aerosol for approximately 4 minutes providing total lung counts of 30,000 cpm for TcO_4^- and at least 10 times background for DTPA. During inhalation respiratory excursions were measured by a spirometer and exhaled particles were trapped in a bacterial filter (Inspiron C.R. Bard, Cucamonga, CA). Scans were done at approximately weekly intervals after irradiation. Of the 10 late sacrifice dogs (see later) - 8 had regular TcO_4^- and DTPA scans, and 2 had only TcO_4^- scans. The early sacrifice dogs had TcO_4^- scans only (see later).

Changes in radioactivity during inhalation and washout were recorded by a gamma camera interfaced to a PDP 11/34 computer system (Digital Equipment Corp., Hudson MA). Clearance was monitored for 40 (1 frame per minute) and 90 minutes (1 frame every 2 minutes) respectively for TcO_4^- and DTPA. Electronically generated regions of interest were drawn onto the lung images to correspond to the right irradiated and left control regions. These regions were defined using radioactive markers superimposed onto tatoo marks as points of reference. Counts were corrected for gamma camera nonuniformity, source decay and background radiation (where necessary) and net clearance curves of activity against time were plotted for the irradiated and control regions. TcO_4^- clearance was mono-exponential and time taken for initial counts to fall by 50% ($t\frac{1}{2}$) was calculated using a non-linear iterative least squares fitting program.(130) The clearance of DTPA proved to be more complex (probably multi-exponential) and was analysed in a manner similar to that of other workers by considering the % fall (in maximum counts) per minute on a linear fit over the first 10 minutes (k). The linear fit was obtained from the computer generated counts, by the method of least squares using a hand held calculator (Hewlett Packard Inc. 10c). The correlation of this linear fit was excellent ($r>0.98$).

(iv) Blood background determination

During the scanning procedure, activity recorded by the gamma camera was the sum of the activities in the airways, alveoli, blood in the lungs and the chest wall. In order to obtain a measure of activity in the alveoli and airways alone, lung and chest wall blood activity was determined by a method modified from that of Jones and co-workers. Briefly, at the end of the scanning procedure, each dog was given approximately 370 MBq of TcO_4^- intravenously. The increase in counts over similar regions drawn in the irradiated and control zones and the heart were then recorded (Figure 10). Ratios (R_B) of the increase in activity over the lung zones to the increase in activity over the heart zone were then determined. These ratios reflected (assuming equal mixing) the ratio of blood in the different zones. Activity in the heart zone during the radioaerosol scan was then multiplied by these ratios to

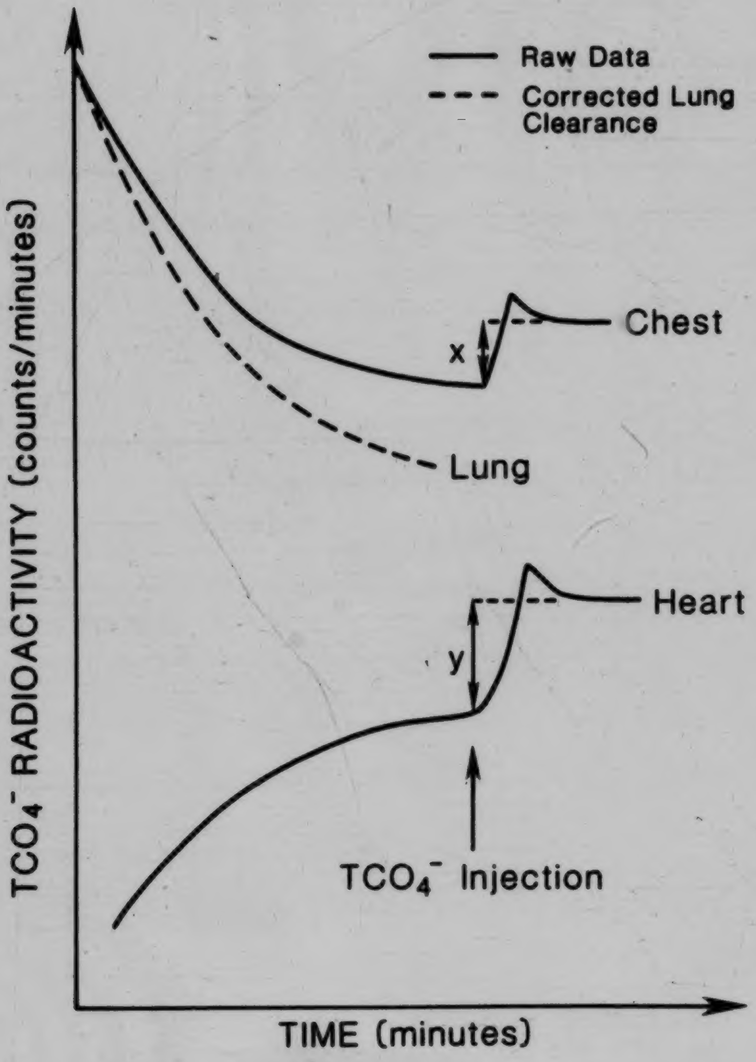

Figure 10 - Determination of blood background. The falling activity in the chest and the rising activity in the heart regions of interest is monitored by a gamma camera. An I.V. bolus of TcO_4^- is given towards the end of the scanning procedure and the ratio of the increase in activities (x/y i.e. R_B) is calculated. This correction factor (R_B x heart region activity, for each minute) can be substracted from chest activity to obtain lung activity alone.

obtain the blood background for each lung zone. The blood background counts could then be subtracted from the original regional clearance curves to obtain activity in the alveoli and airways alone.

(C) Conventional pre-irradiation imaging

(i) Chest radiography

Anesthetized as for scanning, each dog had a supine anterior-posterior chest radiograph. The films were taken using a Picker International System with voltages of 70-80 KEV and 200 MA for 1/10 second. The tube to table distance was 42 inches.

(ii) MAA perfusion scanning

At the end of the scanning procedure, after the determination of blood background, 120 MBq of ^{99m}Technetium macroaggregated albumin (Edmonton Radiopharmaceutical Centre) was given intravenously to each dog. After approximately 3 minutes, the anterior chest was scanned with the gamma camera for 1 minute. A similar static scan was subsequently taken of the right lateral chest.

The MAA perfusion scans were interpreted visually (as is usual in clinical practice) on the basis that a cold area represented obstruction in the vascular bed. In addition, the anterior-posterior scans were interpreted quantitatively in the following manner: Similar sized square regions of interest were drawn in the right irradiated and left control lung zones. The ratio of counts in the irradiated to the control region of interest was then determined for each dog, each week. 95% confidence limits for this ratio was then determined from pre-irradiation scans. Post-irradiation scans were then considered quantitatively abnormal if their ratios fell outside these confidence limits.

(iii) CT scanning

After the pre-irradiation MAA perfusion scans, each dog had a thoracic CT scan (General Electric CT/T 8800). The dog was positioned supine and the sternoclavicular junction aligned to a fixed point on the scanning platform. Six to seven manual hyperinflations (15 ml/kg) were given for one minute prior to scanning in order to attempt to correct any micro-atelectasis that may have resulted during the day's procedures. After the initial "scout scan", transverse sections (1 cm thick) were taken 1.5 cm apart from the lung apices down to the diaphragm. An effort was made to scan between spontaneous breaths but this was often not possible because of the time required for scanning.

The CT scans were interpreted visually by a radiologist (see post-irradiation scanning). In addition, quantitative assessment was made by the measurement of CT number in the following manner: With the "display" level and "window" set at -370 and 100 respectively, the slices in the lower half of the right lung were examined. For each slice a region of interest was drawn in the lung parenchyma excluding large blood vessels but keeping as close as possible to the lung pleura. An average CT number for the parenchyma within the region of interest was then obtained. A CT number was then similarly obtained for each slice in the right lower lung, and the reported number is an overall average of all of these values.

(D) Irradiation

The dogs were anesthetised and prepared as for scanning and the right hemithorax shaved. With the dog supine, a field size of 5 x 7 cm in the right lower lung (approximately 35% of the right lung) zone was simulated. Irradiation was subsequently administered using parallel and opposed fields, from the Cobalt 60 source of a Theratron 780 (Atomic Energy of Canada Ltd.) of effective energy 1.25 Mev. The average dose rate at 80 cm from the source ranged from 100 to 108 CGy/min during the study, with half-value layer of 10.5 mm of lead. The position of the dog during irradiation was maintained by sand bags and taping. Tissue equivalent boluses packed around the chest wall ensured a homogenous radiation field and a dose at mid-plane of 20 Gy. Computer simulation was carried out to verify the homogeneity of dose within the target volume (10%). Treatment times were calculated as detailed in Appendix I. At the end of the procedure the site of irradiation was confirmed by chest radiography and marked on each dog by skin tatoos. Prophylactic intramuscular procaine penicillin (200,000 units) was given at weekly intervals after irradiation.

(E) Post-irradiation imaging

(i) Radioaerosol scanning

TcO_4^- and DTPA radioaerosol scans were performed at weekly intervals after irradiation in the manner previously described. $T\frac{1}{2}$ and k values were compared to those obtained pre-irradiation using the paired student t test. In addition, $t\frac{1}{2}$ and k were considered abnormal if they fell outside their 95% confidence limits calculated from pre-irradiation and control side values. $P<0.05$ was considered significant.

(ii) Blood-background determinations

Blood-background determinations were made at regular intervals in the post irradiation studies, usually on the same days as the radioaerosol scans. The method was as previously described.

The determination of blood-background activity after irradiation was considered to be especially important because if altered, could contribute to a change clearance rates: An increase in blood-background would tend to decrease the clearance rate, and vice-versa.

(iii) Chest radiography

Chest radiographs were taken at weekly intervals after irradiation by the method previously described. They were interpreted visually and compared to normal pre-irradiation radiographs.

(iv) MAA perfusion scanning

MAA perfusion lung scans were performed at regular intervals after irradiation on the same days as the radioaerosol scans, by the method previously described. Comparison of pre and post-irradiation scans were made both by visual inspection and quantitative assessment as described above.

(v) CT scanning

Thoracic CT scans were performed at biweekly intervals after irradiation in the manner previously described. Post-irradiation CT scans were compared to baseline pre-irradiation scans by a radiologist. In order to obtain an objective and unbiased assessment, all the scans were interpreted at the end of the study. At this time scans were given for interpretation randomly and not in chronological order. It was necessary to compare post with pre-irradiation scans because often the pre-irradiation scans had minor changes and post-irradiation scans had to be interpreted taking into account these baseline variations. In addition a quantitative assessment was made using CT number data: using the pre-irradiatin values for CT number in the right lower lung zone for all the dogs, 95% confidence limits were established. The CT number for the right lower lung zone was then considered abnormal if it fell outside this range.

(F) Measurement of lobar compliance

Of the 12 dogs used in this study, two were sacrificed as soon as the TcO_4^- scans became definitely abnormal (early sacrifice dogs). The remaining 10 dogs were sacrificed when all tests were abnormal (late sacrifice dogs).

The dogs were systemically heparinized and sacrificed by rapid desanguination. Midline thoracotomies were performed and the heart and lungs removed intact. The right and left lower lobes were dissected free and used for compliance measurements.

The lobar bronchus was cannulated and the deflation limb of the pressure-volume relationship was examined by the following method: Volume was introduced using a 1 liter calibration syringe and the corresponding pressures measured using a water manometer. The lobe was inflated to maximal lung capacity (volume at 30 cmH_2O inflation pressure) and then deflated. This was repeated three times to establish a volume history and the lobe was then reinflated to 30 cm H_2O pressure. Using the calibration syringe, 40 cc samples of air were sequentially removed and the corresponding airway pressures at each removal noted. This sequence was repeated to obtain 2 sets of data points. On complete deflation (zero airway pressure) the lobe was disconnected and its volume (A) measured by a water displacement method. Minimal gas volume was obtained by subtracting the lobar wet weight from A (assuming the density of tissue and blood to be 1 gm/cc). The compliance of the right and left lower lobes were compared by calculating kc, an index of the exponential function, according to the method of Berend and Thurlbeck.(131) Following the compliance measurements, the left and right lower lobes were placed in formalin and the airways perfused with formalin at 30 cc hydrostatic pressure. This fixation process was continued for 3-5 days.

(G) Morphology

In both the early and late sacrifice dogs, the right lower lobe was sliced into 5 saggital sections after formalin fixation. For the sake of consistency, the mid-saggital slice was used for histology. At least 3 samples were taken from the anterior portion of the slice, one from the mid-portion and one from the posterior portion. Similar corresponding samples were taken from the left lower lobe. Tissue samples were processed for light microscopy using standard techniques and stained with hematoxylin and eosin. The histology was interpreted by a pathologist blinded to the sampling sites.

CHAPTER IV

RESULTS

One of the 10 late sacrifice dogs died 4 weeks after irradiation but unfortunately, the cause of death was not determined. The others maintained their weights and tolerated the procedures well. Hair loss occurred over the area of irradiation.

Radioaerosol scans

Table 3 shows mean values for tidal volume, frequency, calculated minute ventilation and inspiratory flow rate during aerosol inhalation for the dogs during the period of the study.

Visual assessment of aerosol deposition patterns during the scans showed these to be peripheral. No central activity was detected at any point in the scans, and this pattern did not change after irradiation. The lack of central deposition was further confirmed in 2 dogs by a technique used by a number of workers to assess regional particle deposition.(132,133) Briefly sulphur colloid aerosol (with the same technique and similar parameters as TcO_4^-) was given to 2 of the dogs (at 3 weeks post-irradiation). Scans were taken immediately and 22 hours later. After correcting for isotope decay, 22 hours after aerosolization, there were no significant changes in activity over the region of interest, suggesting a lack of mucociliary clearance. (In fact the total count for the right lung appeared to increase after 22 hours, by 11 and 5.3%, respectively in the 2 dogs) This was interpreted as showing that aerosol deposition was mainly peripheral and beyond the mucociliary escalator.

Table 3

VENTILATION PARAMETERS DURING AEROSOLIZATION

Ventilation Parameters	Mean	SE
Tidal volume (cc)	302	6.45
Flow rate (L/min)	16.5	0.5
Frequency (per min)	8.4	0.61
Ventilation (L/min)	2.35	0.19

Blood background

Values for R_B (increase in regional lung activity divided by regional heart activity) for the dogs at various time intervals after irradiation are shown in appendix 2. Weekly variations in R_B were assessed in 6 of these dogs up to 4 weeks post-irradiation by two-way analysis of variance. There was no significant variation in R_B between dogs or between weeks for the right or left sides. Two of these dogs (C504 and C506) were assessed up to 8 weeks after irradiation and values for R_B were similar. In view of the constancy in R_B after irradiation, t ½ and k values were not subsequently corrected for blood background. This was further justifiable in view of the fact that comparison was made only between irradiated and control lung zones at different time intervals after irradiation and not between dogs.

Sodium pertechnetate (TcO_4^-)

The changes in t ½ before and after irradiation for the late sacrifice dogs are illustrated in Figure 11. Prior to irradiation there was no significant difference between right and left side t ½ [Right: 4.11 ± 0.71 min, Left: 4.04 ± 0.78 min (mean ± SD)]. Following irradiation there was no significant change in serial left side t ½, but right side t ½ increased (decreased clearance of TcO_4^-) progressively appearing to reach a plateau at about 8 weeks. The extent of this increase varied from dog to dog, but for all the dogs, the mean t ½ for the right side was significantly greater than mean pre-irradiation t ½ from the second week post-irradiation onwards. Because of the inter-dog variability in right side t ½ following irradiation 95% confidence limits were established for the normal t ½ in individual dogs using pre-irradiation left and right, and post-irradiation left side t ½. The TcO_4^- radioaerosol scan was then considered abnormal in individual dogs when the t ½ exceeded these limits. Figure 12 shows the t ½-time curve for one of these dogs where right side t ½ exceeded the 95% confidence limits at 2 weeks post-irradiation. The normal ranges and times of onset of abnormality in TcO_4^- clearance are shown in Table 4. Using this method of analysis the mean time of onset of abnormal

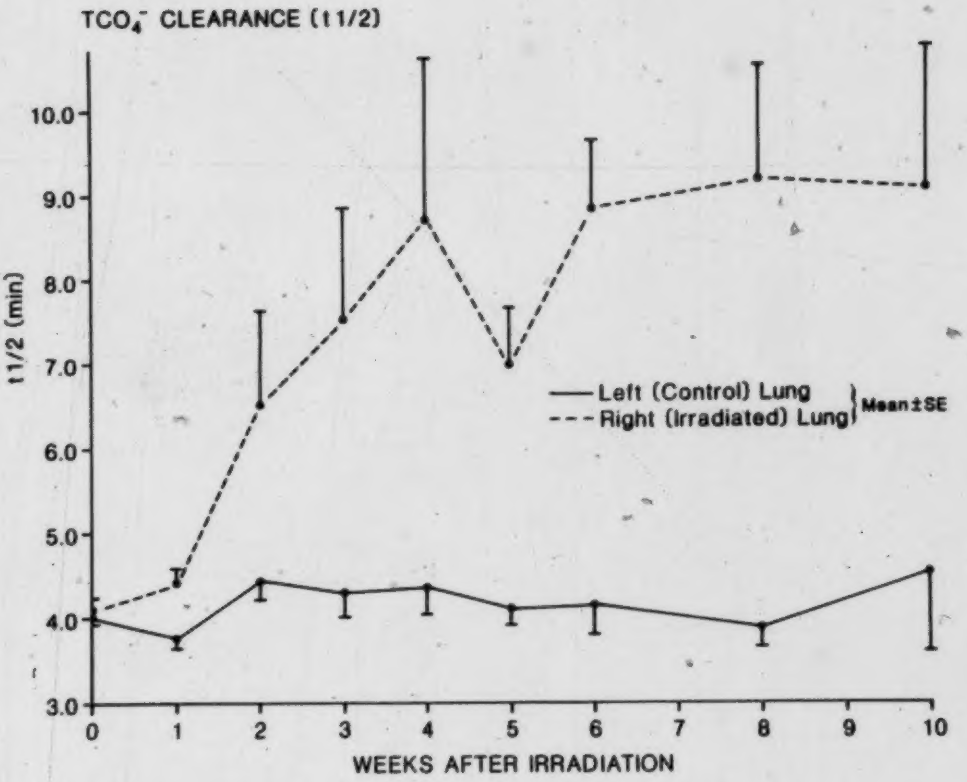

Figure 11 - Changes in the lung clearance of TcO$_4^-$ (t ½) for the right and left lower zones following right lower zone thoracic irradiation.

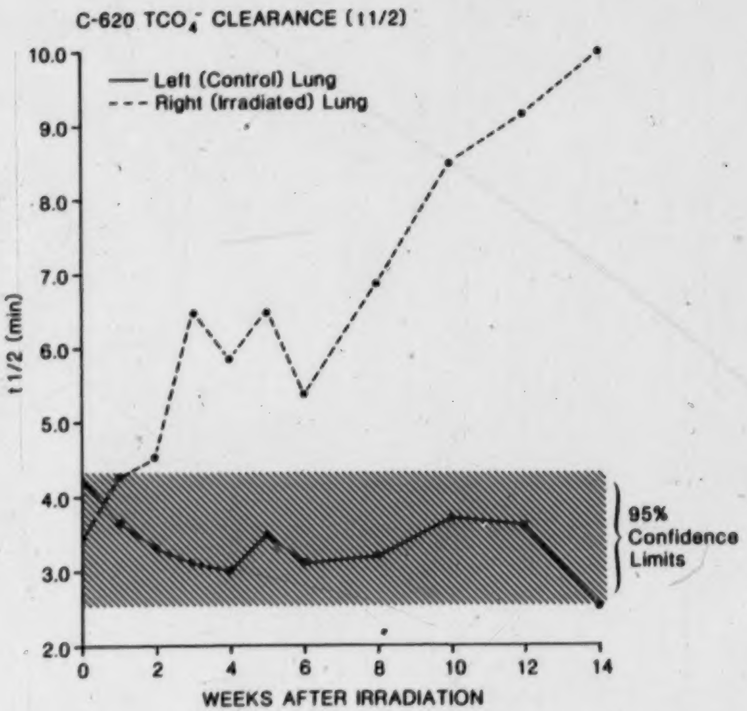

Figure 12 - Changes in the lung clearance of TcO_4^- (t ½) for the right and left lower zones following right lower zone thoracic irradiation in dog C-620. Right side t ½ exceeded the 95% confidence limits at 2 weeks post-irradiation.

Table 4

CONFIDENCE LIMITS FOR TCO_4^- CLEARANCE (t ½) AND THE TIME OF ONSET OF ABNORMALITY

Dog	95% confidence limits for normal t ½ (min)	Onset of abnormality (wks)
C-566	3.2 - 4.7	2
C-526	3.4 - 5.1	2
C-577	3.2 - 4.8	1
C-694	3.0 - 5.0	2
C-620	2.5 - 4.3	2
C-564	3.2 - 6.9	6
C-568	3.7 - 6.7	2
D-119	3.3 - 5.7	3
D-134	2.9 - 5.5	4
C-556*	3.2 - 4.5	2
MEAN	2.7 - 5.7	2.7 ± 1.4

*Died at 4 weeks post-irradiation.

TcO_4^- clearance was determined to be at 2.7 ± 1.4 weeks after irradiation.

Diethylenetriaminepenta-acetate (DTPA)

Before irradiation there was no significant difference between right and left side k (Right: 2.91 ± 0.74 %/min, Left: 3.01 ± 0.98 %/min) (Figure 13). Following irradiation there was no significant change in serial left side k. In

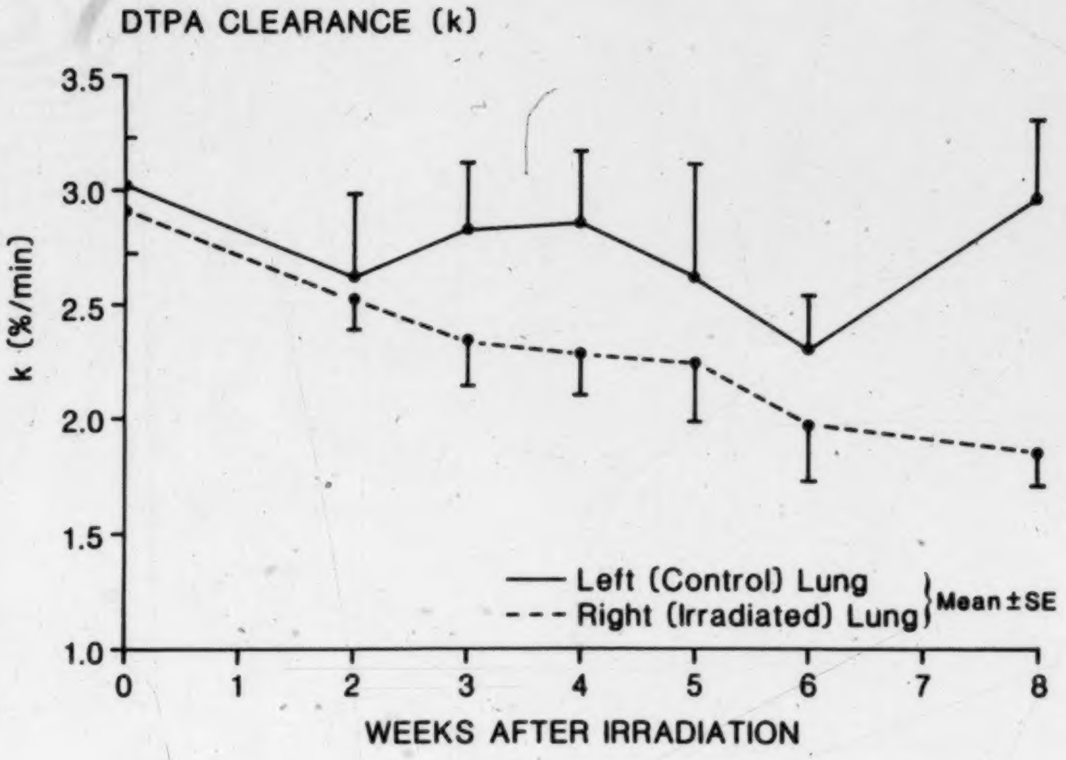

Figure 13 - Changes in lung clearance of DTPA (k %/min) for the right and left lower zones following right lower zone thoracic irradiation in the dogs studied.

contrast, k for the right side decreased (decreased clearance) progressively with time after irradiation. This decrease was not as marked as the increase in TcO_4^- t ½, but when compared to pre-irradiation values was statistically significant from the 2nd week post-irradiation onwards. In individual dogs, although the trend for a decrease in right side k with time was apparent, k fell outside the 95% confidence limits in only 1 dog (C694 at 8 and 9 weeks post-irradiation).

Radiography, MAA perfusion and CT scanning

Abnormalities in chest radiographs and CT scans were seen as density changes in lung parenchyma and/or pleura. In the chest radiographs these changes were always restricted to the irradiated zones, but in the CT scans additional changes were often seen in lower zone slices. These were considered by the radiologist to be due to dilated blood vessels in the gravity dependent regions of the lung. They tended to be symmetrical, in contrast to radiation changes, which when present, were always restricted to the irradiated right lower zone. CT number data were also analyzed quantitatively and the 95% confidence limits for the normal right lower zone pre-irradiation CT number were -692 to -809 (mean = 750; SD = 29). Post-irradiation CT scans were considered abnormal if the right lower zone CT number fell outside this range. When assessed in this manner CT scans were still normal at 8 and 12 weeks respectively in 2 of the dogs (D-134 and C-566)

Table 5

MEAN CT NUMBER FOR THE RIGHT LOWER ZONE AT VARIOUS TIME INTERVALS AFTER IRRADIATION

Weeks after Irradiation	C526	C566	C568	C556$^+$	C564	C620	C577	C694	D134	D119
Pre	-786	-714	-757	-710	-732	-779	-	-	-784	-749
+2									-788	-710
+3			-675*							
+4	-782			-749				-671*	-757	-564*
+5		-723	-515		-682	-728	-732			
+6	-676*	-750			-734	-793	-701		-735	-652
+7								-539	-709	-623
+8		-713			-763	-745	-556*			
+9								-543		
+10		-702			-549*	-690*	-520			
+12						-658				
+14						-515				

* = onset of abnormality.

+ = died at 4 weeks post irradiation.

at a time when visual abnormality had already occurred. (Table 5) The mean time of onset of abnormality in CT scans when assessed visually and quantitatively was 7.1 ± 2.8 weeks and 7.2 ± 3.2 weeks respectively (allowing for convenience that CT number became abnormal in C-566 and D-134 at the next scan). Quantitative CT was not superior to visual CT in this study. Changes in average CT number for the right lower lung zone after irradiation are shown in Table 5 and Figure 14.

In the MAA perfusion scans, abnormalities were seen as areas of reduced perfusion in the irradiated zones. These were analyzed quantitatively and visually. When these scans were interpreted quantitatively the 95% confidence limits (pre-irradiation) for the ratio of counts in the right irradiated zone to the left control zone were 0.86 - 1.46 (mean = 1.16; SD = 0.15). Scans were considered abnormal, post-irradiation, when these limits were exceeded. Analysed in this manner, MAA perfusion scans became quantitatively abnormal at 7.7 ± 3.1 weeks and visually abnormal at 8.0 ± 3.0 weeks (mean ± SD) with no significant difference between the 2 modes of assessment. Table 6 shows the changes in regional count ratios in the MAA scans after irradiation.

The time of onset of abnormality in radioaerosol scans, chest radiographs MAA perfusion (both visual and quantitative) and CT scans (both visual and quantitative) are shown in Table 7. Radioaerosol scan abnormalities

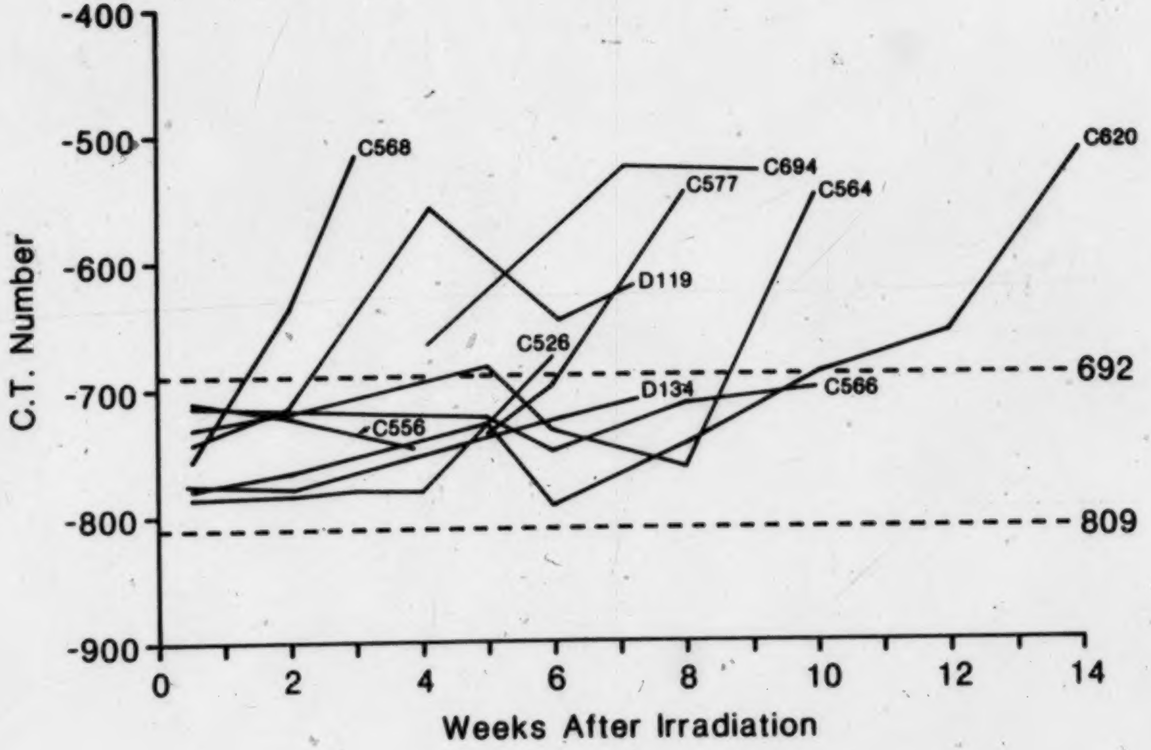

Figure 14 - Changes in average CT number for the right lower zone after irradiation in 10 dogs.

Table 6

CHANGES IN REGIONAL MAA COUNT RATIOS AFTER IRRADIATION AND THE ONSET OF ABNORMALITY

Weeks after irradiation	C566	C526	C577	C694	C620	C564	C568	D119	D134	C556
Pre	0.99	1.29	1.41		1.14	1.1	1.17			1.0
+1										
+2	1.12	0.99		0.94		1.05	0.72			0.96
+3	0.97	0.99	1.6	1.08		0.89	0.90	0.92	0.98	0.97
+4		0.96	1.02	1.09	1.19	1.17	0.62*	0.81*	1.08	1.06
+5	1.14		1.1		1.13	1.15	0.33	0.83		
+6	0.93	0.66*			1.28	0.97		0.76	0.77*	
+7	1.31			1.22		0.81		0.70	0.80	
+8	1.25		0.85*	0.97	1.11	1.29		0.75		
+9	0.42*		0.82	0.82*		1.27				
+10					1.14	0.98				
+11					1.14	0.81*				
+12					0.99					
+13					0.68*					

*Onset of abnormality

Table 7

Dog	Radioaerosol	C.T.		MAA Perfusion		
	(TCO_4^-)	visual	quantitative	visual	quantitative	Cxray
C-566	2	10	12*	9	9	8
C-526	2	6	6	6	6	7
C-577	1	5	8	7	8	10
C-694	2	9	4	9	9	9
C-620	2	10	10	14	13	13
C-564	6	10	10	11	11	10
C-568	2	3	3	4	4	4
D-119	3	4	4	6	4	6
D-134	4	7	8+	6	6	7
MEAN	2.7	7.1	7.2	8.0	7.8	8.2
S.D.	1.5	2.8	3.1	3.0	3.7	2.6

* - still normal at the end of the study (10 weeks) but considered to be abnormal at 12 weeks for analysis.

+ - still normal at the end of the study (7 weeks) but considered to be abnormal at 8 weeks for analysis.

The onset of abnormality (weeks) in various test following thoracic irradiation. See text for details.

occurred significantly earlier (2.7 ± 1.5 weeks) than abnormalities in chest radiographs (8.2 ± 2.6 weeks), MAA perfusion (8.0 ± 3.1 weeks) and CT (7.11 ± 2.8 weeks) scans. In addition there were no significant differences between the times of onset of abnormality in MAA perfusion and CT scans interpreted visually and by quantitative assessment. The biweekly CT scan was superior to chest radiography but MAA perfusion scanning was not.

Lobar compliance

Irradiation of a small volume of lung in our dogs did not significantly alter lobar compliance. The results are summarized in Table 8.

Morphology:

Late sacrifice dogs

At the time of thoracotomy, scarring was clearly visible on the antero-lateral aspects of the right middle and lower lobes. This scarring seemed to be restricted to these sites often involving 1/3 - 1/2 of the surface. (Plate 2) When sliced, fibrotic changes were seen, predominantly in the anterior regions. The extent of this varied, in some dogs involving the full anterior-posterior thickness of the slice and in others merely the pleura and superficial parts of the lobe. Light microscopy showed definite changes of varying degree in samples from the irradiated lobes. Plate 3 illustrates the changes seen in dog C620 - being a

Table 8

COMPLIANCE (Kc) OF THE RIGHT AND LEFT LOWER LOBES AFTER RIGHT LOWER ZONE THORACIC IRRADIATION

Dog	Right Lower Lobe Kc	Left Lower Lobe Kc
C-566	0.10	0.11
C-620	0.07	0.10
C-556	0.11	0.08
C-694	0.08	0.10
C-577	0.08	0.12
C-568	0.05	0.11
C-564	0.10	0.10
C-526	0.11	0.13
D-119	0.09	
D-134	0.11	0.11
MEAN	0.09	0.11
SD	0.02	0.01

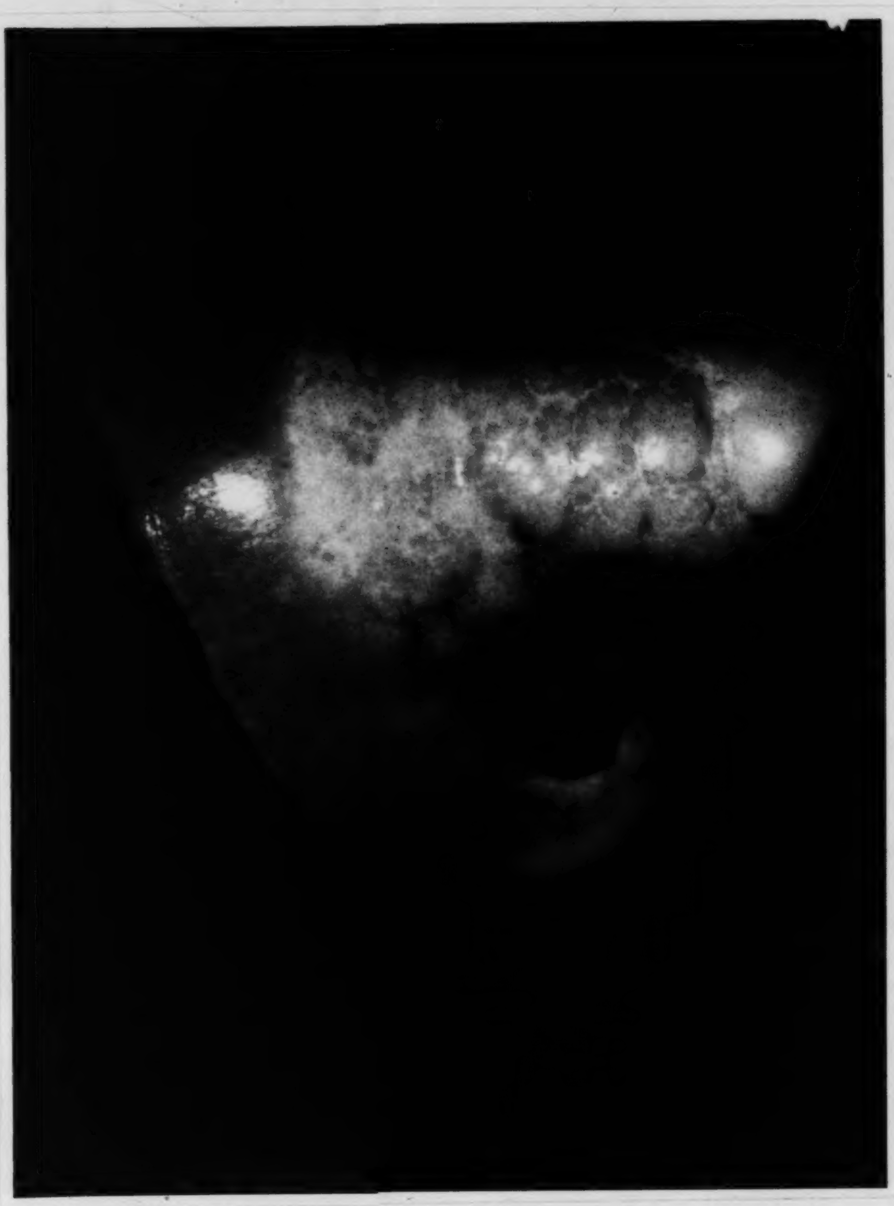

Plate 2 - Excised right lower lobe after thoracic irradiation showing obvious scarring.

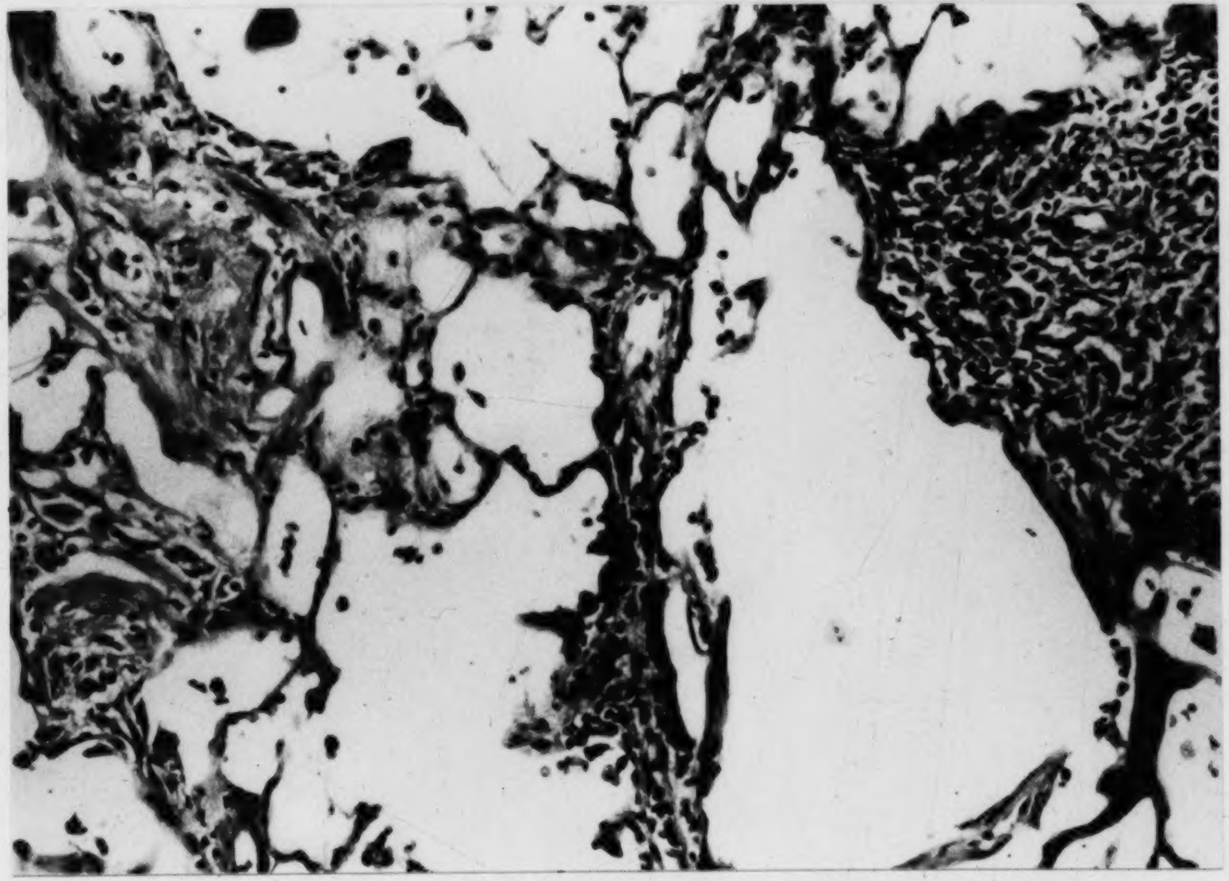

Plate 3 - Changes in light microscopy in the right lower lobe in dog C-620. Appearances are a combination of inflammatory cell infiltration, infra-alveolar exudation and patchy fibrosis.

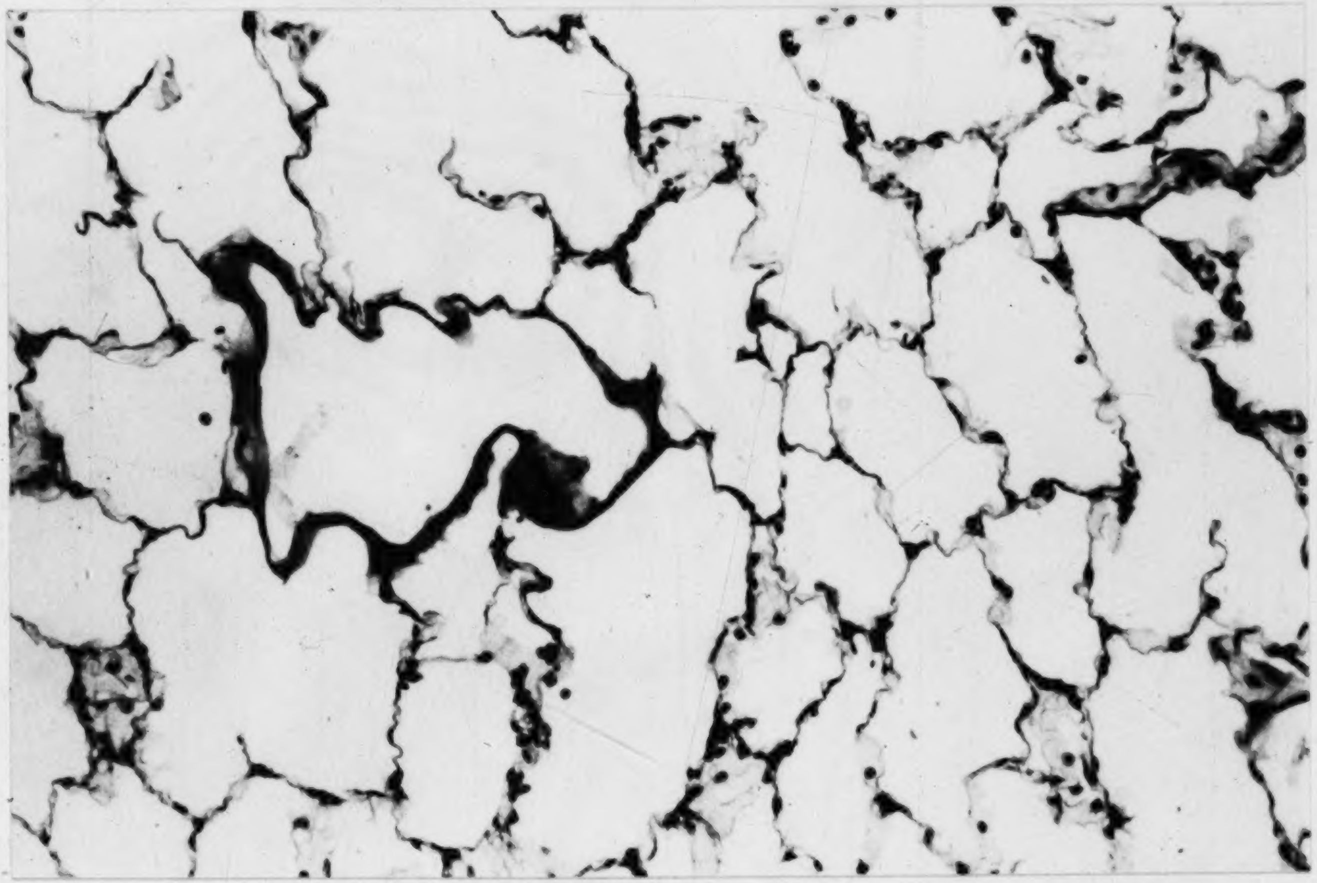

Plate 4 - Section from left lower lobe of dog C-620 showing normal histological appearance.

combination of inflammatory cell infiltration, intra-alveolar exudation and patchy fibrosis. These changes are similar to those described by other workers in radiation pneumonitis. Sections from the non-irradiated lung appeared normal and plate 4 shows a sample from dog C620.

Early sacrifice dogs

The 2 early sacrifice dogs, in which the TcO_4^- radioaerosol scans became abnormal at 1 and 6 weeks post-irradiation respectively, showed no macroscopic lung changes at thoracotomy. Light microscopy showed normal appearances of both right and left lower lobe samples. Plate 5 shows a sample of the right lower lobe from one of the early sacrifice dogs (C730).

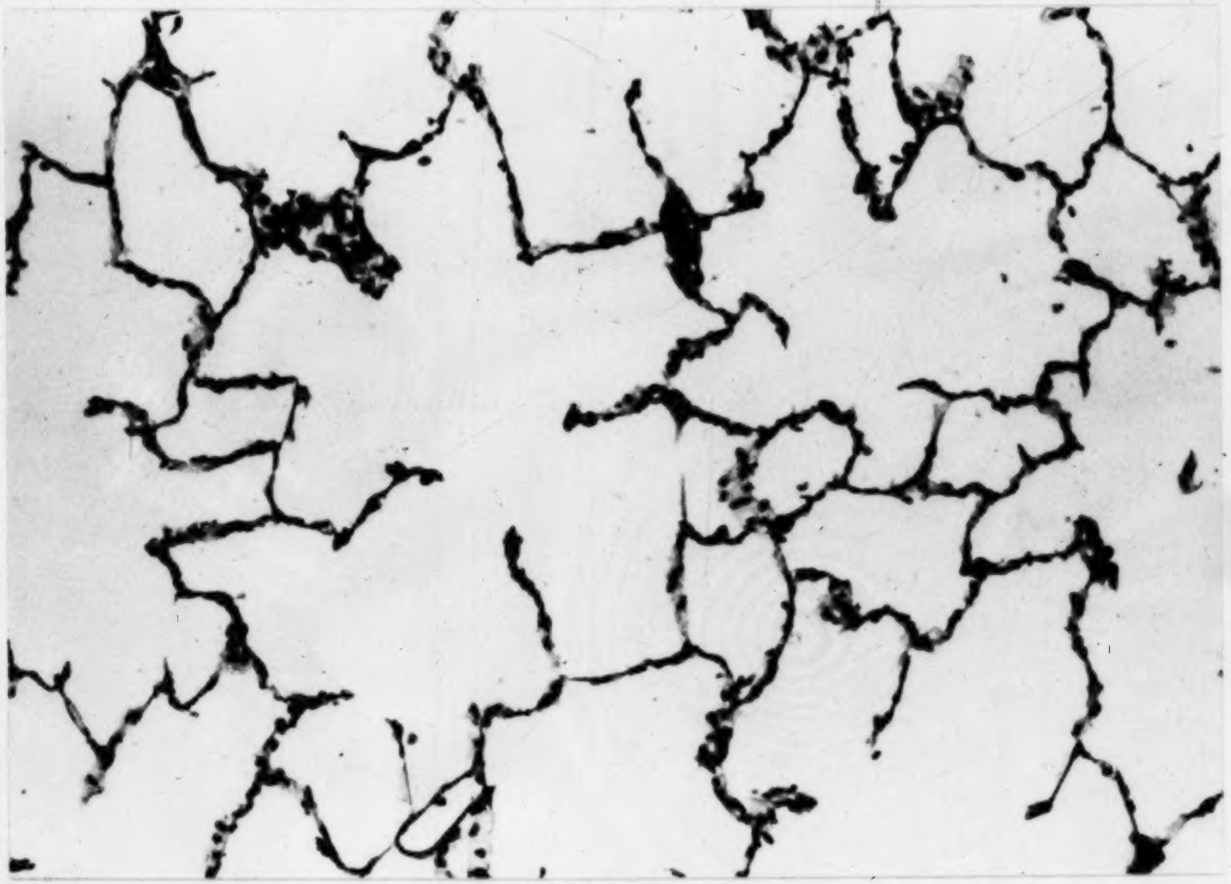

Plate 5 - Section from the right lower lobe of an early sacrifice dog showing normal histology.

CHAPTER V

DISCUSSION

Our results show that approximately 2 weeks after thoracic irradiation in dogs there is a significant reduction in the alveolar to capillary clearance of both TcO_4 and DTPA. This alteration occurs at a time when lung histology (in 2 early sacrificed dogs), chest roentgenograms, MAA perfusion and computerized tomographic (CT) lung scans are still normal. Solute clearance rates continue to fall after irradiation whilst chest roentgenograms, MAA perfusion and CT scan do not become abnormal until 8.2 ± 2.6, 8.0 ± 3.1, and 7.1 ± 2.8 weeks post-irradiation respectively. By the time the earliest imaging abnormality occurs (C.T. at 7.1 weeks) TcO_4^- and DTPA clearance have fallen by approximately 125 and 63 percent respectively. At sacrifice, (mean = 8 ½ weeks post-irradiation) all dogs show changes compatible with radiation pneumonitis but lobar compliance is not altered. The preservation of normal lobar compliance was most likely because of the small volume of lung irradiated.

The sequence of changes outlined above and the consistency of these findings in all dogs together with the eventual lung damage documented by histology strongly suggests that the changes in solute clearance were due to the effects of thoracic irradiation.

Technical factors which may have biased our results, e.g. alteration in aerosol deposition patterns after irradiation, and changes in blood background were not thought to have occurred, and these are considered in more detail below. Impaired mucociliary transport is unlikely to have played a significant part in the clearance of the solutes for a number of reasons. Firstly, it is well accepted that particles of the size used in our studies are mainly deposited beyond the mucociliary escalator in the non-ciliated alveolar regions.(132,134-136) In addition, two dogs given aerosolized sulphur colloid showed no significant change in regional counts (after decay correction) after 22 hours. This finding together with the lack of central activity at any point in our scans and a rate of solute clearance much faster than is possible by mucociliary transport, confirm that the latter mechanism was probably not operative in our studies. The rates of solute clearance seen were also much faster than those reported for lymphatic and alveolar macrophage transport.(137) It is thus most likely that the particles were cleared by translocation across the alveolar-capillary membrane into the pulmonary circulation. As mentioned in the literature review numerous workers have in fact used this radioaerosol scanning technique to measure alveolar-capillary membrane permeability (pulmonary permeability) and have shown increases in permeability in cigarette smokers,(99) and in patients with systemic sclerosis,(96) interstitial lung disease(97) and asthma.(111) In our study, an increase in blood background after irradiation may theoretically have been responsible for the reduction in solute clearance seen. However blood background did not change after irradiation and the increase in regional lung counts divided by the increase in heart count (R_B) following pertechnetate injection remained fairly constant with no significant variation up to 4 weeks after irradiation.

In contrast to lipid soluble molecules which traverse the epithelia rapidly and are limited by perfusion, the passage of hydrophilic solutes (such as those used in our study) is limited by diffusion. As such, the rate of solute diffusion (dQ/dt) through the membrane is directly proportional to surface area for transfer (S) and the concentration gradient across the membrane (dc/dx) in accordance with Fick's first law of diffusion,

$$dQ/dt = -DS\ dc/dx$$

where D represents the diffusion coefficient of a given solute. In addition, the diffusion of a solute is inversely related to the diffusion distance or thickness of the membrane (dx). Thus a reduction in the rate of transfer for a given solute across the alveolar-capillary membrane may be due to an increase in diffusion distance, a fall in the concentration gradient across the membrane or a decrease in the surface area for transfer. Translocation of solutes across the air-blood barrier is also dependent on molecular size. This is compatible with a diffusive mechanism for transfer. DTPA is a much larger molecule than TcO_4^- and this probably accounts for the separate pathway it takes as well as its slower translocation rate. The increase in clearance of DTPA in guinea pigs exposed to cigarette smoke has been shown by cytochemical techniques to be due to a widening of the tight junctions between cells.(115) DTPA translocation is therefore most likely via the tight junctions, and is restricted in the alveolar epithelium and capillary endothelium by the size and frequency of tight junctions TcO_4^- probably crosses passively both across cells and via the paracellular pathway. No active mechanism has yet been confirmed for either solute. For solute particles which are deposited in the alveoli, Fick's first law of diffusion applies to each of the component parts of the alveolar-capillary membrane, i.e. alveolar lining fluid, alveolar epithelium, interstitium and capillary endothelium. Values of $t\frac{1}{2}$ and k represent an overall measure of membrane permeability, but clearly in radiation lung injury some components may be affected more than others.

In trying to determine the mechanisms responsible for the reduced alveolar clearance of solutes in radiation lung injury it is useful to examine the effects of radiation on each of the components of the air-blood barrier. One of the most consistent features of radiation lung injury seen both in our studies and in others is a thickening of the whole alveolar-capillary membrane,(6,120) increasing the diffusional distance. This thickening affects all components of the barrier. The alveolar surface is lined by proteinaceous exudate and often also by the hyaline membranes once thought to be pathognomonic of radiation lung injury.(1) The edema fluid may reduce clearance by increasing the diffusion distance. However, Mason et al(109) have paradoxically shown an increase in the clearance of aerosolized DTPA in patients with non-hemodynamic pulmonary edema. It is therefore unlikely that alveolar edema alone causes the reduction in solute clearance seen in our studies. Binding of TcO_4^- or DTPA to albumin reducing its clearance is also unlikely because clearance rates are much faster than those possible for a pertechnetate-albumin complex, on size criteria alone. However, partial binding with a resulting decrease in clearance is still a possibility. Rinderknecht and colleagues,(97) using a similar radioaerosol scanning procedure found a reduced clearance of TcO_4^- in 4 patients with pulmonary alveolar proteinosis (PAP). In this condition the alveoli are filled with a thick eosinophilic granular material containing large amounts of lipoid.(138) They reported that clearance of TcO_4^- returned towards normal in two of these patients after lavage. They mention no data on DTPA. Thus in radiation pneumonitis, although the proteinaceous edema fluid may not be enough to reduce the clearance of the solutes, the addition of the hyaline membranes may be such as to do this in a manner similar to that in patients with PAP. The thickening of alveolar lining fluid probably affects the diffusional transfer of TcO_4^- and DTPA equally. The thickness of the alveolar epithelium is increased by edema, fibrosis and the invasion of histocytes and fibroblasts. Translocation of DTPA probably occurs only at the tight junctions, whilst TcO_4 crosses via both the cellular and transcellular routes. A thickening of the epithelium is therefore likely to impede translocation of TcO_4^- more than that of DTPA unless the tight junctions are also narrowed. There is an increase in the interstitial tissue and this probably reduces the diffusion of both solutes equally. The effects of radiation on the capillary endothelium are varied. Initially, there is swelling of the endothelial cells with eventual sloughing and blockage of capillary lumen. Some workers have suggested an increase in vascular permeability due to disruption of the endothelial cells. At a later stage there is repair with recanalization of the lumen and fibrous thickening of the endothelial wall. The translocation of TcO_4^- and DTPA across the endothelium may therefore vary depending on the stage of lung injury. Taylor and Garr(34) using the concept of reflection coefficients showed that the tight junctions within the alveolar epithelium are 5-8 times tighter than those in the capillary endothelium. The alveolar epithelium is therefore the limiting barrier of the alveolar-capillary membrane. It is clear therefore, that if the alterations responsible for the reduced clearance resides in the epithelium or endothelium, the epithelium must be more greatly affected for the overall permeability to fall. Diamond(139) has related the t ½ for build-up or decay of solute across a membrane to diffusion coefficient (D) and membrane thickness (C) by the formula:

$$t\,{}^1\!/_2 = 0.38\ C^2/D$$

If the whole alveolar-capillary membrane is considered as one, and D is assumed constant, simple manipulation of the above equation shows that a doubling of $t\,{}^1\!/_2$ can be produced by a 40% increase in membrane thickness. In our study pre-irradiation $t\,{}^1\!/_2$ equalled approximately 4 min and this increased to approximately 6.5 min at 2 weeks, the first occasion when the increase was statistically significant. This increase in $t\,{}^1\!/_2$ corresponds to a 28% increase in membrane thickness, a change which is clearly very conceivable. It is highly likely therefore that a thickening of the alveolar capillary membrane plays a part in the reduced clearance of solutes seen in radiation lung damage. DTPA is less affected than TcO_4 possibly because the thickening does not affect its passage through the tight junctions.

A reduction in surface area for transfer is another factor which could reduce solute translocation rate. Surface area for transfer (s) is clearly different for TcO_4^- and DTPA; TcO_4 has the whole alveolar wall available for diffusion, whereas DTPA is restricted to the tight junctions. Malfunction of pulmonary surfactant is considered to be the primary cause of alveolar collapse in early radiation lung injury.(2) This reduction in alveolar wall surface area could theoretically impede TcO_4 flux but quantitation is difficult. At the present time no objective data exists, to our knowledge, to show reduction in surface area for transfer in radiation injury. A reduction in diffusion capacity ($D_{L_{CO}}$) is a common finding in the intermediate stages but this could equally well be due to ventilation-perfusion mismatch. For TcO_4^-, a reduction in alveolar wall surface area due to collapse probably affects all components of the air-blood barrier equally. Effros and Mason(35) have recently argued that in aerosol studies, more important than surface area in controlling the rate of solute translocation is the ratio of permeability surface area product (ps) to volume (v). They suggest that if the intrinsic permeability of the epithelium remains constant and surface area (s) and v change by equivalent degrees, the rate of solute translocation will not be altered. In radiation lung injury, therefore, a reduction in flux can only occur in this context, if s decreases more than v. This is theoretically possible if the alveolar wall were naturally convoluted, and with radiation this convolution decreases, thereby reducing surface area, but leaving alveolar volume intact. A more likely explanation, however, is a fall in permeability (p). For DTPA, surface area for transfer primarily depends on the alveolar epithelium which forms the limiting barrier and the number, frequency and patency of its tight junctions. Alveolar distension by increasing lung inflation has been shown to progressively increase alveolar-capillary membrane permeability until maximal distention when even protein molecules can traverse.(105,106) This has been considered to be due to stretching open of the tight junctions between cells. The converse, i.e. a narrowing of the tight junctions with alveolar collapse, thereby reducing solute flux has not been shown, and is probably unlikely. Because the alveolar epithelium acts as the limiting barrier, it is easy to see how changes in the capillary endothelium, which may themselves increase permeability, do not increase overall flux unless the alveolar wall is similarly damaged.

Despite the fact that aerosol deposition in our studies was mostly alveolar, it is probable that some was terminal bronchiolar and clearance rates probably reflect bronchiolar as well as alveolar-capillary membrane permeability. It is unknown whether the permeability characteristics of the bronchiolar epithelium differ from those of the flat alveolar epithelium. However, the far greater area of the alveolar epithelium probably mean that any contribution that the bronchiolar epithelial permeability gives to the overall permeability is small.

The final consideration regarding the diffusion process is the concentration gradient of solute (dc/dx) across the membrane. This probably applies to both TcO_4 and DTPA although their pathways are different. In the normal situation the rapid flow of blood in the pulmonary circulation maintains a high transmembrane concentration gradient. Slowing of blood flow and in the extreme case stagnation may reduce this, possibly resulting in a decrease in clearance. It is probable however, that extreme decreases of blood flow (<1% of normal) would be required to produce this.(97) Many workers have shown that lung irradiation leads to hypoperfusion of the irradiated zones(140-142) and this has been used as one of the early indices of radiation lung injury. Similar changes were observed in our studies and the mean onset of these changes was at 8.0 ± 3.1 weeks post-irradiation (Table 7). At the time of onset of the reduced solute clearance, however, there was no change in the MAA perfusion scan and blood background remained fairly constant throughout the study excluding stagnation of blood in the irradiated zones. It is therefore unlikely that the reduced clearance of TcO_4 and DTPA was due to a reduced concentration gradient brought on by changes in alveolar blood flow. Accumulation of solute in the interstitium without passage into the pulmonary circulation is another possibility that could both simulate a reduced clearance on the gamma camera images and reduce the concentration gradient across the membrane. Despite its theoretical possibility, there is no evidence that it occurs, and it seems unlikely.

Despite fairly convincing evidence in our study for a reduced alveolar-capillary membrane permeability Gross has shown in a study on irradiated mice(143) that there is an increase in the flux of ^{125}I-labeled albumin from capillary to alveolus. He examined both alveolar lavage samples and homogenised lung and found that 4 months after 30 Gy to the thorax, when compared to control mice, there was a five fold increase in lavage protein and that lung homogenate also contained more protein. There were no significant increases in alveolar protein at 2 months after irradiation. Henderson and co-workers(144) in a study on beagle dogs also found increases in protein flux by the 28th day after 60 Gy. It therefore seems likely that radiation leads to an increase in translocation of albumin from capillary to alveolus. On face value their results appear to contradict ours. However the 2 studies are examining different things: the solutes, pathways and directions of flux are all different. Our study examines flux from alveolus to capillary whereas the other studies are capillary to alveolus. The other studies look at albumin flux which probably occurs transcellularly by pinocytosis (in normal tissue) whilst our studies are concerned with TcO_4^- and DTPA which traverse by the transcellular route directly and via the paracellular pathway. Any measurement of alveolar-capillary membrane permeability must therefore consider bidirectional flux and pathway, as well as solute used. Another difference between the studies of Gross, Henderson et al and ours is that increased flux of albumin was not seen until 4 months after 30 Gy (Gross) and 28 days after 60 Gy (Henderson). In our studies we showed a decrease in flux of solutes at 2 weeks after 20 Gy. It is possible that had we followed our dogs for much longer or given larger doses of radiation, we would have noticed an increase in solute flux. However, we have followed one dog to 6 months after

20 Gy and 2 dogs to 4 weeks after 40 Gy and found persistent decreases in solute flux (unpublished observations). Regardless of these considerations, albumin does appear to get into the alveoli. Gee and Staub have suggested(77) that in hemodynamic pulmonary edema, alveolar flooding occurs, not directly through the alveolar wall, but along high conductance pathways through the epithelium of the broncho-alveolar junction. It is conceivable that the same process occurs in radiation lung injury so that although alveolar epithelial permeability is reduced, albumin can enter the interstitium through the damaged capillary endothelium and then pass indirectly into the alveolus via breaks in the bronchiolar epithelium.

Clearly much more work has to be done to answer these questions. On balance it seems most likely that in radiation lung injury the permeability of the alveolar capillary membrane to TcO_4^- and DTPA is reduced from the alveolar to capillary side. Although structural changes in the membrane and alterations in surface area may play a part, the most likely explanation is a thickening of the alveolar capillary membrane by fibrous tissue and hyaline membranes. Albumin flux from capillary to alveolus may be increased at a later stage but possibly via a different pathway involving the terminal bronchiolar wall.

To date the diagnosis of radiation pneumonitis, in the clinical situation, has been largely based upon symptomatology, physical examination and chest radiography. Although some idea of the risks of developing pneumonitis can be ascertained from the radiation dose and schedule used, there is still great variability in response between patients on similar radiation schedules. The onset of symptoms and abnormalities in chest radiography always occurs after a latent interval although it is likely that damage occurs at the time of radiation exposure.(2) At the present time no noninvasive method exists to adequately assess this early damage. The need to quantify lung changes following radiation is seen by the significant morbidity and mortality in pneumonitis and the fact that the radiation tolerance of the lung represents the limiting factor in thoracic irradiation schedules. If a test existed which could document lung injury at an early stage and predict the likelihood of pneumonitis, thoracic irradiation schedules could be used more effectively. Moreover an index of lung injury generated from this test could be used in studies to assess prevention and treatment. The changes in lung function which occur after radiation have been well described by a number of workers. They include a reduction in lung volumes, lung compliance, diffusing capacity and regional blood flow.(145-147) The time of onset of these changes depends on the radiation dose and volume of lung irradiated. Although Emirgil and Heinemann(145) have shown that many of these changes occur before the onset of radiological abnormalities, the physiological changes still occur relatively late. In their study, for example, in which patients with various thoracic malignancies were given 25-50 Gy over 21-72 days, abnormalities did not occur until 43-1390 days post-radiation. Sweany and co-workers(146) found no changes in lung compliance, steady-state diffusing capacity and FRC up to 4 weeks after 10-29 Gy to the mid-chest in dogs. Prato(147) found significant alterations in regional lung function, especially blood flow, in patients given radiotherapy for breast carcinoma. However these changes occurred between 3 months and 6 years after radiation. In the clinical setting, the definitive test for radiation pneumonitis is lung biopsy, but this would probably be difficult to justify until radiological changes were apparent.

Experimental work with xenon and MAA have shown that hypoperfusion of the irradiated lung zones is a common feature of radiation lung injury.(140-142,147) In our study however the perfusion lung scan was not able to detect lung injury any earlier than the chest radiograph. Goldman and co-workers in a study on humans came to a similar conclusion.(140)

There has been considerable recent interest in the use of CT scanning in the early detection of radiation lung injury.(150) Besides the obvious visual interpretation of lung changes, the assessment of lung density by the use of CT number has been thought to be of particular value. Although densities in g/cm^3 can be approximated from CT number by the relationship

$$\text{physical density} = \frac{\text{CT number}}{1000} + 1 \text{ gm/cm}^3$$

raw CT numbers can more easily be used to assess physical densities.(148) The density of lung parenchyma is determined both by the density of lung tissue per se and the relative quantities of fluid and air within the lung. Rosenblum and co-workers(148) showed that lung density, as measured by CT number, is lower at higher lung volumes, and that dependent parts of the lung are more dense because of gravity induced pooling of blood. Medlund et al(149) found that lung density decreased during hemorrhagic shock due to reduced pulmonary blood volume - but returned towards normal after resuscitation. In a study on oleic acid induced pulmonary edema(149), Medlund and colleagues were also able to document increases in lung density due to increasing interstitial edema. El-Khatib and co-workers(150), found an increase in lung density, as assessed by CT number, in mice irradiated with 10 Gy or more. All these studies suggest that CT numbers can be used as an accurate and fairly sensitive measure of lung density both in normals and in disease states.

In our studies the biweekly CT scan interpreted visually was able to detect radiation induced changes significantly earlier than chest radiography. If done weekly it would probably have been superior, statistically at least, than MAA perfusion scanning. Having described the value of CT densitometry it is very disappointing that in our studies assessmsent of density changes by CT number did not provide a better way of diagnosing abnormality than did visual assessment. However this was probably due to technical difficulties inherent in the method of calculating CT number. The measurement of CT number was done on lung parenchyma, so the pleura which is often involved in radiation injury was not included. Visual examination on the other hand, did allow pleural changes to be taken into account, and in this respect was superior. In addition, difficulties arose in drawing the regions of interest because of the need to exclude major blood vessels. Moreover, the CT number obtained was an average of the CT numbers in all the pixels of the region of interest (rather than just in the damaged zone) and this tended to reduce the sensitivity of the test. The CT numbers reported in this study were means of the CT numbers for the right lower zone slices thereby further "diluting" the results.

The TcO_4^- radioaerosol scan was able to detect lung injury considerably earlier (2.7 ± 1.5 weeks) than Cxray (8.2 ± 2.6), MAA (8.0 ± 3.1) or CT (7.2 ± 2.8) scans. It is interesting to note that there were no changes in light microscopy in the early sacrifice dogs even though clearance of TcO_4^- was altered. Although we did not perform physiological tests during the study, compliance of the right lower lobes were not altered.

The ability to assess regional changes in clearance is a great advantage of the radioaerosol scan and makes it superior to D_LCO. The diffusion capacity test although appearing similar to the radioaerosol scan has important differences. The diffusion of carbon monoxide across the alveolar-capillary membrane is dependent primarily upon the extent of the capillary bed and hemoglobin level and insensitive to changes in the tight junctions and the thickness of the alveolar-capillary barrier. The radioaerosol scan is very sensitive to changes in the tight junctions and the thickness of the alveolar-capillary barrier and largely insensitive to changes in blood flow and possibly surface area.

The radioaerosol scan is easy to perform and certainly within the capabilities of most major hospitals. Further studies are required to assess if the technique can detect changes in permeability in humans and at lower doses of radiation. It would also be important to know if abnormal clearance rates reverse with resolution of pneumonitis. The technique has potential value in the early assessment of radiation lung injury and in combination with D_LCO it may provide complete information on the functional integrity of the alveolar-capillary membrane.

CHAPTER VI

SUMMARY AND CONCLUSIONS

This study has shown that in radiation lung injury in dogs, there is a reduction in the pulmonary permeability for TcO_4 and DTPA from the alveolar to capillary side. This occurs at approximately 2 weeks after 20 Gy to the right lower lung zone and is probably due to a thickening of the effective alveolar-capillary membrane. The TcO_4^- scan is able to detect changes significantly earlier (2.7 ± 1.5 weeks) than chest radiography (8.2 ± 2.6 weeks) MAA perfusion (8.0 ± 3.1 weeks) and CT (7.1 ± 2.8) scanning. That these changes are related to radiation lung injury is shown by the persistence of abnormal TcO_4^- clearance and the finding of morphological features of radiation pneumonitis at the time of sacrifice approximately 8 ½ weeks post-irradiation. Further studies are required, however, to determine the specificity of the test and to see if there is a correlation between reduced aerosol clearance and morphology. If substantiated in human studies and at therapeutic doses and schedules of radiation, the TcO_4^- scan may have potential value in the early detection of radiation lung injury.

REFERENCES

1. Groover T.A., Christie A.C., Merritt E.A. Observations on the use of the copper filter in the roentgen treatment of deep-seated malignancies. South Med. J. 1922; 15: 440-444.

2. Gross N.J. The pathogenesis of radiation induced lung disease. Lung 1981; 159: 115-125.

3. Moss W.T., Haddy F.J., Sweany S.K. Some factors altering the severity of acute radiation pneumonitis: variation with cortisone, Heparin and antibiotics. Radiology 1960; 75: 50-54.

4. Castellino R.A., Glatstein E., Turbow M.M. et al. Latent radiation injury of lungs or heart activated by steroid withdrawl. Ann. Intern. Med. 1974; 80: 593-599.

5. Phillips T.L. An ultrastructural study of the development of radiation injury in the lung. Radiology 1966; 87: 49-54.

6. Warren S. and Spencer J. Radiation reaction in the lung. Am. J. Roentgen. 1940; 43: 682.

7. Moosavi H., McDonald S., Rubin P., Cooper R., Stuard D. and Penney D. Early radiation dose-response in lung: an ultrastructural study. Int. J. Radiation Onc. Biol. Phys. 1977; 2: 921-931.

8. Leroy E.P., Liebner E.J., Jensik R.J. The ultrastructure of canine alveoli after supervoltage irradiation of the thorax. Lesions of the latent period. Lab. Invest. 1966; 15(10): 1544-1558.

9. Faulkner C.S., Connolly K.S. The ultrastructure of ^{60}C radiation pneumonitis in rats. Lab. Invest. 1973; 28(5): 545-553.

10. Penney D.P. and Rubin P. Specific early fine structural changes in the lung following irradiation. Int. J. Radiation Onc. Biol. Phys. 1977; 2: 1123-1132.

11. Travis E.L., Harley R.A., Fenn J.O., Klobukowski C.J. and Hargrove H.B. Pathological changes in the lung following single and multi-fraction irradiation. Int. J. Radiation Onc. Biol. Phys. 1977; 2: 475-490.

12. Schneeberger E.E., Structural basis for some permeability properties of the air-blood barrier. Fed. Proc. 1978; 37: 2471-2478.

13. Gross N.J. Pulmonary effects of radiation therapy. Ann. Intern. Med. 1977; 86: 81-92.

14. DeFouw D.O. Ultrastructural features of alveolar epithelial transport. Am. Rev. Respir. Dis. 1983; 129(Supp): S19-S13.

15. Cottrell T.S., O.R. Levine, R.M. Senior, W. Joseph, D. Spiro, and A.P. Fishman. Electron microscopic alterations at the alveolar level in pulmonary edema. Circulation Res. 1967; 21: 783-798.

16. Weibel E.R. Morphometric estimation of pulmonary diffusion capacity. V. Comparative analysis of mammalian lungs. Respir. Physiol. 1972; 14: 26-37.

17. Meban, C. Thickness of the air-blood barriers in vertebrate lungs. J. Anat. 1980; 131: 299-307.

18. Weibel E.R. **Morphometry of the human lung.** New York: Academic. 1963; p.101.

19. Mazzone R.W., Kornblau S.M. Pinocytotic vesicles in the endothelium of rapidly frozen rabbit lung. Microvasc. REs. 1981; 21: 193-211.

20. Gill J., Silage D.A. Morphometry of pinocytotic vesicles in the capillary endothelium of rabbit lungs using automated equipment. Circ. Res. 1980; 47: 384-91.

21. Schneeberger E.E. Ultrastructural basis for alveolar-capillary permeability to protein. In: Porter M., O'Connor R., eds. Lung liquids, Ciba foundation symposium 38. Elsevier/ Excerpta Medica/North - Holland 1976, p.3.

22. Michel R.P., Inoue S., Hogg J.C. Pulmonary capillary permeability to HRP in dogs; a physiological and morphological study. J. Appl. Physiol. 1977; 42: 13-21.

23. Boucher R.C., Johnson J., Inoue S., Hulbert W., Hogg J.C. The effect of cigarette smoke on the permeability of guinea pig airways. Lab Invest. 1974; 31: 75-81.

24. Rinderknecht J., Shapiro L., Krauthammer M., et al. Accelerated clearance of small solutes from the lungs in interstitial lung disease. Am. Rev. Respir. Dis. 1980; 121: 105-17.

25. Weibel E.R. Morphometric estimation of pulmonary diffusion capacity. Respir. Physiol. 1970/1971; 11: 54-75.

26. Sorokin S.P. A morphological and cytochemical study on the great alveolar cell. J. Histochem. Cytochem. 1966; 14: 884-897.

27. Petrik P. Fine ultrastructural identification of peroxisomes in mouse and rat bronchiolar and alveolar epithelium. J. Histochem. Cytochem. 1971; 19: 339-348.

28. Schneeberger E.E. A comparative cytochemical study of microbodies (peroxisomes) in great alveolar cells of rodents, rabbit and monkey. J. Histochem. Cytochem. 1972; 20: 180-191.

29. Chevalier G., Coller A.J. In vivo incorporation of choline - ^{3}H, Leucine-^{3}H and galacose-^{3}H in alveolar type II pneumocytes in relation to surfactant synthesis: a quantitative radioautographic study in mouse by electron microscopy. Anat. Rec. 1972; 174: 289-310.

30. Smith F.B., Kikkawa Y. The type II epithelial cells of the lung III. Lecithin Synthesis: a comparison with pulmonary macrophages. Lab. Invest. 1978; 38: 45-51.

31. Adamson I.Y.R., Bowden, D.H. The type II cell as a progenitor of alveolar epithelial regeneration. Lab. Invest. 1974; 30: 35-42.

32. Chinard F.P. The permeability characteristics of the alveolar capillary barrier. Trans. Assoc. Am. Physicians 1962; 75: 253-61.

33. Taylor A.E., Guyton A.C., Bishop V.S. Permeability of the alveolar membrane to solutes. Circ. Res. 1967; 16: 353-62.

34. Taylor A.E., Garr K.A. Estimation of equivalent pore radii of pulmonary capillary and alveolar membranes. Am. J. Physiol. 1970; 218: 1133-40.

35. Effros R.M. and Mason G.R. Measurements of pumonary epithelial permeability in vivo. Am. Rev. Respir. Dis. 1983; 127(Supp): S59-S65.

36. Vaccaro C.A., Brody J.C. Structural features of the alveolar wall basement membrane in the adult rat. J. Cell Biol. 1981; 91: 427-37.

37. Brenner B.M. Hostetler T.H., Humes H.D. Molecular basis for proteinuria of glomerular origin. N. Engl. J. Med. 1978; 298: 826-33.

38. Morgan T.E. Pulmonary surfactant. N. Engl. J. Med. 1971; 284: 1185-93.

39. Scarpelli E.M., Wolfson D.R. and Colacicco G. Protein and lipid: protein frations of lung washings. Immunological characteristics. J. Appl. Physiol. 1973; 34: 750-753.

40. Weibel E.R., Gil J. Electron microscopic demonstration of an extra-cellular duplex lining layer of alveoli. Respir. Physiol. 1968; 4: 42-57.

41. Frömter E., Diamond J. Route of passive ion permeation in epithelia. Nat. New Biol. 1972; 53: 9-13.

42. Frömter E. The route of passive ion movement through the epithelium of Necturus gallbladder. J. Membr. Biol. 1972; 8: 259-301.

43. Machen T.E., Erlij D., Wooding F.B.P. Permeable junctional complexes: the movement of lanthanum across rabbit gallbladder and intestine. J. Cell Biol. 1972; 54: 302-12.

44. Erlij D., Martinez-Palomo A. Role of tight junctions in epithelial function. In: Giebrisch G., Tosteson D.C., Ussing H.H., eds. Membrane transport in biology, Vol. III. Berlin: Springer-Verlag 1978: 27-53.

45. Schneeberger E.E. and Karnovsky M.J. Substructure of intercellular junctions in freeze fractured alveolar-capillary membranes of mouse lung. Circ. Res. 1976; 38: 404-411.

46. Bradley S.E., Purcell E.F., eds. The paracellular pathway. New York: Tosiah Macy Jr. Foundation, 1982, pp 1-382.

47. Simionescu M., Simionescu N. and Palade G.E. Segmental differentiations of cell junctions in the vascular endothelium. The microvasculature. J. Cell Biol. 1975; 67: 863-885.

48. Claude P. and Goodenough D.A. Fracture faces of zonulae occludentes from "tight" and leaky" epithelium. J. Cell Biol. 1973; 58: 390-400.

49. Inoue S., Nickel R.P., and Hogg J.C. Zonulae occludentes in alveolar epithelium and capillary endothelium of dog lungs studied with the freeze fractured technique. J. Ultrastruct. Res. 1976; 56: 215-225.

50. Claude P. Morphological factors influencing transepithelial permeability: A model for the resistance of the zonula occludens. J. Membr. Biol. 1978; 39: 219-32.

51. Van Deurs B., Koehler J.K. Tight junctions in the choroid plexus epithelium. J. Cell Biol. 1979; 80: 662-73.

52. Wright E.M. Mechanisms of ion transport across the choroid plexus. J. Physiol. (London) 1972; 226: 545-571.

53. Olver R.E. and Strang L.B. Ion fluxes across the pulmonary epithelium and the secretion of lung liquid in the fetal lamb. J. Physiol. (London) 1974; 241: 327-357.

54. Brindslev N., Wright E.M. A thermodynamic analysis of nonelectrolyte permeation across the toad urinary bladder. J. Membr. Biol. 1976; 29: 265-88.

55. Casaburi R., Wasserman K., Effros R.M. Detection and measurement of pulmonary edema. In: Staub N.C., ed. Lung, water and solute exchange. New York: Marcel Dekker, 1978; 323-63.

56. Schneeberger E.E. and Karnovsky M.J. The influence of intravascular fluid volume on the permeability of newborn and adult mouse lung to ultrastructural protein tracers. J. Cell Biol. 1971; 49: 319-334.

57. Bignon J., Chahinian P., Feldman G. and Sapin C. Ultrastructural immunoperoxidase demonstration of autologous albumin in the alveolar capillary membrane and in the alveolar lining material in normal rats. J. Cell Biol. 1975; 64: 503-590.

58. Sapin C. and Warnet J.M. Immunoelectron microscopic and immunochemical demonstrations of serum proteins in the alveolar lining material of the rat lung. Am. Rev. Respir. Dis. 1976; 113: 109-120.

59. Landis E.M. and Pappenheimer J.R. Exchange of substances through capillary walls. In: Handbook of Physiology, Sect.2: Circulation, Vol.2 edited by W.F. Hamilton and P. Dow. Washington, D.C. Am. Physiol. Soc. 1963; p.961-1034.

60. Michel C.C. Direct observation of the sites of permeability for ions and small molecules in mesothelium and endothelium. In: Capillary permeability, edited by C. Crone and N.A. Lassen. Copenhagen, Munksgaard 1970; p.628-642.

61. Brindslev N., Tormey J. McD, Pietras R.J., Wright E.M. Electrically and osmotically induced changes in permeability and structure of toad urinary bladder. Biochim. Piophys. Act. 1974; 332: 286-97.

62. Cereijido M., Meza I. The control of tight junctions in tissue culture. In: Bradley S.E., Purcell E.F., eds. The paracellular pathway. New York: Josiah Macy Jr. Foundation 1972; 83-94.

63. Schneeberger E.E. and Karnovsky M.J. The ultrastructural basis of alveolar-capillary membrane permeability to peroxidase used as a tracer. J. Cell Biol. 1968; 37: 781-793.

64. Schneeberger E.E. and Karnovsky M.J. The influence of intravascular fluid volume on the permeability of newborn and adult mouse lung to ultrastructural protein tracers. J. Cell Biol. 1971; 49: 319-334.

65. Pietra G.G., Szidon J.P., Levanthal M.M. and Fishman A.P. Hemoglobin as a tracer in hemodynamic pulmonary edema. Science 1969; 166: 1643-1646.

66. Theodore J., Robin E.D., Gaudio R. and Acevedo J. Transalveolar transport of large polar solute (sucrose, inulin, and dextran). Am. J. Physiol. 1975; 229(4): 989-996.

67. Wright E.M., Pietras R.J. Routes of nonelectrolyte permeation across epithelial membranes. J. Membr. Biol. 1974; 17: 293-312.

68. Smulders A.P., Wright E.M. The magnitude of nonelectrolyte selectivity in the gallbladder epithelium. J. Membr. Biol. 1971; 5: 297-318.

69. Kim K.J., Crandall E.D. Heteropore population of bullfrog alveolar epithelium. J. Appl. Physiol. 1983; 54: 140-6.

70. Wright E.M. Solute and water transport across epithelia. Am. Rev. Respir. Dis. 1983; 127(supp): S3-S8.

71. House C.R. Water transport in cells and tissues. London: Edward Arnold Ltd. 1974; p.1-562.

72. Diamond J.M. Osmotic water flow in leaky epithelia. J. Membr. Biol. 1979; 51: 195-216.

73. Zeuther T., Wright E. Epithelial potassium transport: Tracer and electrophysiological studies in choroid plexus. J. Membr. Biol. 1981; 60: 105-28.

74. Saito Y., Wright E.M. Kinetics of the Na pump in the frog choroid plexus. J. Physiol. 1982; 328: 229-43.

75. Nelson R.M., McDityre B.R., Egan E.A. Solute permeability of the alveolar epithelium in alloxan edema in dogs. J. Appl. Physiol. 1978; 44: 353-7.

76. Zumsteg T.A., Havill A.M., Gee M.H. Relationship among lung extravascular fluid compartments with alveolar flooding. J. Appl. Physiol. 1982; 53: 267-71.

77. Gee M.H., Staub N.C. Role of bulk fluid flow in protein permeability of the dog lung alveolar membrane. J. Appl. Physiol. 1977; 42: 144-9.

78. Yoneda K. Regional differences in the intercellular junctions of the alveolar-capillary membrane in the human lung. Am. Rev. Respir. Dis. 1982; 126: 893-897.

79. Olver R.E., Davis B., Marin M.G. and Nadel J.A. Active transport of Na^+ and Cl^- across the canine tracheal epithelium in vitro. Am. Rev. Respir. Dis. 1975; 112: 811-815.

80. Gatzy J.T. Ion transport across the excised bullfrog lung. Am. J. Physiol. 1975; 228: 1162-1171.

81. Enna S.J., Schanker L.S. Phenol red absorption from the rat lung: evidence of carrier transport. Life Sci. 1973; 12: 231-9.

82. Gardiner T.H., Goodman F.R. Comparison of uptake and binding of disodium cromoglycate and phenol red in rat lung. J. Pharmacol. Exp. Ther. 1976; 198: 395-402.

83. Man S.F.P., Ahmed I.H. Man G.C.W. an Nguyen A. Use of Na-$^{99m}TcO_4$ to explore Cl^- channels in canine airway epithelium. Clinical and Investigative Medicine 1983; 6(supp 2): 78.

84. Chinard F.P. The alveolar-capillary barrier. Some data and speculations. Microvasc. Res. 1980; 19: 1-17.

85. Taylor A.E., Guyton A.C., Bishop V.S. Permeability of the alveolar membrane to solutes. Circ. Res. 1964; 16: 353-362.

86. Wangensteen O.D., Wittmers L.E. Jr., Johnson J.A. Permeability of the mammalian blood-gas barrier and its components. Am. J. Physiol. 1969; 216(4): 719-727.

87. Egan E.A. Fluid balance in the air-filled alveolar space. Am. Rev. Respir. Dis. 1983; 127: S37-S39.

88. Staub N.C. Pulmonary edema. Physiol. Rev. 1974; 54: 678-811.

89. Staub N.C. Pulmonary edema due to increased microvascular permeability for fluid and protein. Circ. Res. 1978; 43: 143-51.

90. Staub N.C. Pulmonary edema due to increased microvascular permeability. Ann. Rev. Med. 1978; 32: 291-312.

91. Brigham K.L., Owen P. and Bowers R. Increased permeability of sheep lung vessels to proteins after pseudomonas bacteriemia. Microvas. Res. 1976; 11: 415-419.

92. Wasserman K., Loeb L. and Mayerson H. Capillary permeability to macromolecules. Circ. Res. 1979; 45: 292-297.

93. Jones J.G., Berry M., Hulands G.H., Crawley J.C. The physiology of leaky lungs. Br. J. Anaeth. 1982; 54: 705-21.

94. Grossman R.F., Fern A., Jones J.G., Little J.W., Hoeffel J., McKay D. Adrenalin-induced alteration in alveolar capillary membrane permeability. Am. Rev. Respir. Dis 1979; 119: 373.

95. Fein A., Grossman R.F., Jones J.G., Hoeffel J., McKay D. Carbon monoxide effect on alveolar epithelial permeability. Chest 1980; 78: 726-31.

96. Chopra S.K., Taplin G.V., Tashkin D.P., Elam D. Lung clearance of soluble aerosols of different molecular weights in systemic sclerosis. Thorax 1979; 34: 63-67.

97. Rinderknecht J., Shapiro L., Krauthammer M., Taplin G., Wasserman K., Uszler J.M., and Effros R.M. Accelerated clearance of small solutes from the lungs in interstitial lung disease. Am. Rev. Respir. Dis. 1980; 121: 105-117.

98. Chan T.L., Lippman M. Experimental measurements and empirical modelling of the regional deposition of inhaled particles in humans. Am. Ind. Hyg. Assoc. J. 1980; 41: 399-408.

99. Jones J.G., Minty B.D., Lawler P., Hulands G., Crawley J.C.W., Veau N. Increased alveolar epithelial permeability in cigarette smokers. Lancet 1980; 1: 66-8.

100. Jones J.G., Royston D. and Minty B.D. Changes in alveolar-capillary barrier function in animals and humans. Am. Rev. Respir. Dis. 1983; 127(supp): S51-S59.

101. Jones T.G., Milay B.D., Beeley J.M., Royston D., Crow J., Grossman R.F. Pulmonary epithelial permeability is immediately increased after embolisation with oleic acid but not with neutral fat. Thorax 1982; 37: 169-85.

102. Jones J.G., Minty B.D., Needham J., Royston D. Effect of sex, age and weight on an index of pulmonary epithelial permeability in Sprague-Dawley rats. J. Physiol. (Lond) 1982; 328: 65-66.

103. Rizk N.W., Luce J.M., Price D.C., Hoeffa J., Murray J.F. Factors influencing clearance of aerosolized ^{99}Tc-diethylenetriaminepentaacetate (^{99m}TcDTPA) from canine lungs. Physiologist 1982; 25: 313.

104. Egan E.A., Olver R.E., Strang L.B. Changes in non-electrolyte permeability of alveoli and the absorption of lung liquid at the start of breathing in lamb. J. Physiol. (London) 1975; 244: 161-79.

105. Egan E.A., Nelson R.M., Olver R.E. Lung inflation and alveolar permeability to non-electrolytes in the adult sheep in vivo. J. Physiol. (London) 1976; 260: 409-24.

106. Egan E.A. Response of alveolar epithelial solute permeability to changes in lung inflation. J. Appl. Physiol. 1980; 49: 1032-36.

107. Egan E.A. Lung inflation, solute permeability and alveolar edema. J. Appl. Physiol. 1982; 55: 121-5.

108. Kim K.J., Crandall E.D. Effects of lung inflation on alveolar epithelial solute and water transport properties. J. Appl. Physiol. 1982; 52(6): 1498-1505.

109. Mason G.R., Uszler J.M. and Effros D.M. Differentiation between hemodynamic and nonhemodynamic pulmonary edema by a scanning procedure. Am. Rev. Respir. Dis. 1981; 123: 238.

110. Anderson R.R., Holliday R.L., Driedger A.A., Lefcoe M., Reid B. and Sibbald W.J. Documentation of pulmonary capillary permeability in the adult respiratory distress syndrome accompanying human sepsis. Am. Rev. Respir. Dis. 1979; 119: 869-877.

111. O'Byrne P.M., Dolovich M., Duvall A., Newhouse M.T. Lung epithelial permeability after histamine challenge. Am. Rev. Respir. Dis. 1982; 125: 280.

112. Elwood R.K., Kennedy S., Belzberg A., Hogg J.C. and Pare P.D. Respiratory mucosal permeability in asthma. Am. Rev. Respir. Dis. 1983; 128: 523-527.

113. Hulbert W.C., Walker D.C., Jackson A., Hogg J.C. Airway permeability in horseradish peroxidase in guinea pigs: the repair phase after injury by cigarette smoke. Am. Rev. Respir. Dis. 1981; 123: 320-6.

114. Minty B.D., Jordan C., Jones J.G. Rapid improvement in abnormal pulmonary epithelial permeability after stopping cigarettes. Br. Med. J. 1981; 282: 83-6.

115. Simani A.S., Inoues, Hogg J.C. Penetration of the respiratory epithelium of guinea pigs following exposure to cigarette smoke. Lab. Invest. 1974; 31: 75-81.

116. Jones J.G., Minty B.D., Royston D., Royston J.P. Carboxyhemoglobin and pulmonary epithelial permeability in man. Thorax 1983; 38: 129-33.

117. Minty B.D., Royston D., Jones J.G. The effect of nicotine on pulmonary epithelial permeability in man. Thorax 1982; 37: 791.

118. Hines L.E. Fibrosis of the lung following roentgen-ray treatments for tumor. JAMA 1922; 79: 720-722.

119. Tyler A.F., Blackman J.R. Effect of heavy radiation on pleurae and lungs. J. Radiol. 1922; 3: 469-475.

120. Rubin P., Casarett G.W. Clinical radiation pathology Vol.1. W.B. Saunders Co., Philadelphia 1968; p.423-591.

121. Maisin J.R. The ultrastructure of the lung of mice exposed to a supra-lethal dose of ionizing radiation on the thorax. Radiat. Res. 1970; 44: 545-564.

122. Maisin J.R. The influence of radiation on blood vessels and circulation III. Ultrastructure of the vessel wall. Curr. Top. Radiat. Res. Q. 1974; 10: 29-57.

123. Adamson I.Y.R., Bowden D.H., Wyatt J.P. A pathway to pulmonary fibrosis: an ultrastructural study of mouse and rat following radiation to the whole body and hemithorax. Am. J. Pathol. 1970; 58: 481-498.

124. Phillips T.L., Benak S., Ross G. Ultrastructural and cellular effects of ionizing radiation. Front. Radiat. Ther. Oncol. 1972; 6: 21-43.

125. Madrazo A., Suzuki Y., Churg J. Radiation pneumonitis, ultrastructural changes in the pulmonary alveoli following high doses of radiation. Arch. Pathol. 1973; 96: 262-268.

126. Watanabe S., Watanabe K., Ohishi T et al. Mast cells in the rat alveolar septa undergoing fibrosis after ionizing radiation. Lab. Invest. 1974; 31: 555-567.

127. Jennings F.L., Arden A. Development of experimental radiation pneumonitis. Arch. Pathol. 1961; 71: 437-446.

128. Goldenberg V.E., Warren S., Chute R. et al. Radiation pneumonitis in single and parabiotic rats. Lab. Invest. 1968; 18: 215-226.

129. Engelstad R.B. Pulmonary lesions after roentgen and radium irradiation. Am. J. Roentgen. 1940; 43: 676-681.

130. Metzler C.M., Elfring G.L., McEwen A.J. Nonlin. A package of computer programs for pharmacokinetic modeling. Biometrics: September 1974; 30: 3.

131. Berend N., Thurlbeck W.M. Exponential analysis of pressure-volume relationship in excised human lungs. J. Appl. Physiol. 1982; 52(4): 838-844.

132. Lourenco R.V., Klimek M.F., Burowski C.J. Deposition and clearance of 2 μ particles in the trachobronchial tree of normal subjects - smokers and non-smokers. J. Clin. Invest. 1971; 50: 1411-20.

133. Lippmann M., Albert R.E. The effect of particle size on the regional deposition of inhaled aerosols in the human respiratory tract. Am. Ind. Hyg. Assoc. J. 1969; 30: 257-75.

134. Chan T.L., Lippmann M. Experimental measurements and empirical modelling of the regional deposition of inhaled particles in humans. Am. Ind. Hyg. Assoc. J. 1980; 41: 399-408.

135. Taplin G.C., Chopra S.K. Inhalation lung imaging with radioactive aerosols and gases. In: Guter M. Ed. Progress in Nuclear Medicine Vol. 5 Basel, Muncher, Paris, London, New York, Sydney: S. Karger, 1978; 119-43.

136. Morrow P.E., Gibb F.R., Gazioglu K.M. A study of particulate clearance from the human lungs. Am. Rev. Respir. Dis. 1967; 96: 1209-21.

137. Lauweryns J.M., Baeat J.H. Alveolar clearance and the role of the pulmonary lyphatics. Am. Rev. Respir. Dis. 1977; 115: 625-683.

138. Rosen S.H., Castleman B., Liebow A.A. Pulmonary alveolar proteinosis. N. Engl. J. Med. 1958; 158: 1123.

139. Diamond J.M. A rapid method for determining voltage concentration relations across membranes. J. Physiol. (Lond) 1966; 183: 83-100.

140. Korsower J.M., Skovron M.L., Nemetallah A.G. and Goldman H.S. Acute changes in arterial perfusion following irradiation. Radiology 1971; 100: 691-693.

141. Freedman G.S., Lotgren S.B., Kugerman M.M. Radiation induced changes in pulmonary perfusion. Radiology 1974; 112: 435-437.

142. Slavson D.O., Fletcher F.H., and Chiffelle T.L. The pulmonary vascular pathology of experimental radiation pneumonitis. Am. J. Pathol. 1977; 88: 635-654.

143. Gross N.J. Experimental radiation pneumonitis IV: leakage of circulatory proteins onto the alveolar surface. J. Lab. Clin. Med. 1980; 95: 19-31.

144. Henderson R.F., Muggenburg B.A., Mauderly J.L. and Tuttle W.A. Early damage indicators in the lung: time sequence of protein accumulation and lipid loss in the airways of beagle dogs with beta irradiation of the lung. Radiat. Res. 1978; 76: 145-158.

145. Emirgil G., Heinemann H.O. Effects of irradiation of chest on pulmonary function in man. J. Appl. Physiol. 1961; 16(2): 331-338.

146. Sweany S.K., Moss W.T., Haddy F.J. The effects of chest irradiation on pulmonary function. J. Clin. Invest. 1959; 38: 587-593.

147. Prato F.S., Kurdyak R., Saibil E.A., Rider W.D., Aspin N. Regional and total lung function in patients following pulmonary irradiation. Investigative Radiol. May-June 1977; 12(3): 224-237.

148. Rosenblum L.J., Mauceri R.A., Wellenstein D.E. et al. Density patterns in normal lung as determined by computed tomography. Radiology 1980; 137: 409-416.

149. Medlund L.W., Effmann E.L., Bates W.M., Beck I.W., Goulding P.L., Putman C.E. Pulmonary Edema: A CT study of regional changes in lung density following oleic acid injury. J. Comput. Assist. Tomogr. 1982; 6(5): 939-946.

150. El-Khatib E., Sharplin J., Battista J.J. The density of mouse lung in vivo following X-irradiation. Int. J. Radiat. Oncol. Biol. Phys. 1982; 9: 853-858.

APPENDICES

Appendix 1

Calculation of irradiation time:

$$\text{Time per beam} = \frac{\text{Mid-plane dose per field}}{\text{dose rate} \times \text{CC} \times \text{PF} \times \text{TAR} \times \text{LCF}} + \text{SC}$$

CC = coning correction

PF = perspex correction

SC = shutter correction

TAR = Tissue-air ratio (at half anterior-posterior separation)

LCF = Lung-correction factor (Batho)

Assuming chest wall = Ccm, the geometric lung path is

$$L = s/2 - C.$$

Assuming lung density of 0.33, the correction in lung is:

$$\text{LCF} = (\text{TAR})^{-0.67}$$

The treatment time is recalculated for the posterior beam because of a different perspex factor.

Appendix 2a

BLOOD-BACKGROUND (R_B) AFTER IRRADIATION

Weeks after	C564		C556		C620		C566	
irradiation	R	L	R	L	R	L	R	L
Pre	0.56	0.66	0.62	0.53	0.58	0.52	0.53	0.52
1					0.43	0.46		
2	0.56	0.47	0.58	0.44	0.52	0.49	0.59	0.59
3	0.57	0.50	0.48	0.49	0.59	0.51	0.53	0.55
4	0.49	0.48	0.47	0.55	0.66	0.49	0.61	0.51
5	0.60	0.49			0.66	0.58	0.51	0.57
6	0.57	0.42			0.63	0.52	0.59	0.59
7	0.55	0.49					0.55	0.51
8	0.47	0.43					0.45	0.49

Appendix 2b

BLOOD-BACKGROUND (R_B) AFTER IRRADIATION

Weeks after	C568		C526		C577	
irradiation	R	L	R	L	R	L
Pre	0.46	0.53	0.54	0.51	0.51	0.46
1					0.51	0.35
2	0.52	0.56	0.68	0.55	0.53	0.35
3	0.53	0.56			0.72	0.60
4	0.68	0.67	0.54	0.46	0.66	0.55
5						
6			0.60	0.39	0.70	0.65

Appendix 3a

SUMMARY OF TCO_4^- DATA

Weeks after	C566		C564		C694		C577		C556	
irradiation	R	L	R	L	R	L	R	L	R	L
-2	4.29+	4.09	5.17	5.09	4.17	4.04	3.95	4.12	4.30	4.28
-1	3.65	4.25	3.67	6.91	4.04	3.82	4.75	4.61	3.67	3.54
+1					4.18	3.75	4.80*	3.95		
+2	6.26*	4.28	5.85	4.48	5.06*	4.02	5.34	4.36	4.54*	3.61
+3	5.43	3.26	6.85	6.11	4.74	4.42	6.88	3.61	5.92	3.73
+4	5.07	3.95	6.38	4.88	5.24	3.55	7.78	3.73	5.31	3.78
+5	6.58	3.95	5.85	4.26			9.97	3.87		
+6	8.65	4.31	7.51*	5.19	8.94	5.38	9.99	3.70		
+7										
+8	5.61	4.08	8.82	4.50	12.08	3.75	12.40	3.70		
+9					13.27	3.56				
+10	5.86	3.59					8.12	3.52		

* Earliest onset of abnormality.

+ Numbers are $t_{1/2}$ for TcO_4^- clearance in min.

Appendix 3b

SUMMARY OF TCO_4^- DATA

Weeks after	C620		D134		D119		C568		C526	
irradiation	R	L	R	L	R	L	R	L	R	L
-2	3.33+	4.08	3.88	4.05	4.20	3.95	4.70	4.28	4.66	4.65
-1	3.51	4.38	3.14	3.41	3.81	3.98	6.60	5.25	4.78	4.28
+1	4.23	3.62								
+2	4.54*	3.32	4.78	5.16	5.15	4.61	15.60*	5.74	6.08*	3.92
+3	6.44	3.11	5.30	4.51	6.01*	4.96	17.79	4.77	8.26	3.75
+4	5.82	3.00	7.79*	4.89	6.60	5.95	23.65	4.95	10.12	4.48
+5	6.48	3.44	7.87	4.27	5.41	4.63				
+6	5.38	3.10	9.47	4.52	7.42	4.53			13.24	3.66
+8	6.99	3.21	9.84	5.29	5.48	3.98				
+10	8.54	3.73	9.09	4.25						
+12	9.19	3.61	15.09	3.76						
+14	10.02	2.49								

* Earliest onset of abnormality

+ Numbers are $t\,{}^1\!/_2$ for TcO_4^- clearance in min.

Appendix 4a

SUMMARY OF DTPA DATA

Weeks after	C566		C564		C694		C577	
irradiation	R	L	R	L	R	L	R	L
-2	3.63+	5.56	2.28	2.09	2.88	3.50	2.56	2.72
-1	4.38	3.91	3.79	4.07			1.90	1.64
+1					2.49	2.85	1.88	2.48
+2	2.98	2.80	2.37	2.54	2.46	2.03	2.18	1.52
+3	3.44	5.35	2.30	2.20	2.58	2.44	1.92	2.58
+4	2.36	2.70	2.75	2.80	2.76	2.76	1.65	2.96
+5	2.87	2.06	2.09	2.12			1.72	2.08
+6	2.10	2.38	2.37	1.81	1.98	2.44	1.06	1.74
+8	1.85	2.49	1.66	2.13	1.64	2.98	1.74	3.04
+9					1.53	2.62		
+10							1.50	2.54

+ Numbers are k % fall/min over the first 10 min.

Appendix 4b

SUMMARY OF DTPA DATA

Weeks after	C556		C620		C526		C568	
irradiation	R	L	R	L	R	L	R	L
-2	3.86	2.75	3.88+	3.54	2.63	2.88	2.41	2.88
-1	3.56	2.95	2.68	2.32	2.38	4.30	2.86	2.31
+1			2.29					
+2	2.75	2.56	2.78	3.04	2.81	4.47	1.83	1.94
+3	2.35	2.94	2.18	3.08	1.80	3.08	2.10	2.10
+4			2.27	3.64	1.96	2.30		
+5			2.33	4.22				
+6			2.40	3.07				
+8			2.38	4.16				
+9								
+10			2.52	3.22				
+12			2.68	4.43				

+ Numbers are k % fall/min over the first 10 min.

CURRICULUM VITA

NAME: Iqbal Hussein Ahmed

DATE OF BIRTH: December 30, 1953

PLACE OF BIRTH: Kampala, Uganda

NATIONALITY: British

EDUCATION: Kent College, Canterbury, Kent.
Manchester Medical School, ENGLAND

EXAMINATIONS:

M.B., Ch.B.	1977
Visa qualifying examination (USA)	1979
M.R.C.P. (UK)	1981
L.M.C.C.	1983

AWARDS:

Alberta Heritage Foundation for Medical Research Fellowship	1982-83
Alberta Lung Association Research Fellowship	1982-83

POSTGRADUATE TRAINING:

Jan 1984 - present - Senior Medical Resident, Dept. of Medicine, University of Alberta, Edmonton.

July 1982 - Dec 1983 - Research fellow, Division of Pulmonary Diseases, Dept. of Medicine, University of Alberta.

July 1981 - June 1982 - Clinical fellow, Division of Pulmonary Diseases, Dept. of Medicine, University of Alberta.

March 1980 - Feb 1981 - Senior Medical House Officer, St. Bartholomews Hospital, London EC2

Jan 1979 - Feb 1980 - Senior Medical House Officer, The Prince of Wales Hospital, London.

Feb 1978 - Aug 1978 - Medical House Officer, Hope Hospital (University of Manchester), Salford, Lancashire.

Aug 1977 - Jan 1978 - Surgical House Officer, Bury General Hospital, Bury, Lancs.

PUBLICATIONS

Abstracts

+(1) Radioaerosol scanning compared to conventional imaging techniques in radiation lung injury. IH Ahmed, W Logus, GCW Man, E El-Khatib, J Battista, SFP Man. Chest 1983; 84: 323.

(2) An early index of radiation induced lung damage. IH Ahmed, W Logus, GCW Man, E El-Khatib, J Battista, SFP Man. Am. Rev. Respir. Dis. 1983; 127: 143.

(3) Radioaerosol scanning in radiation lung injury. IH Ahmed, W Logus, GCW Man, SFP Man. Clinical and Investigative Medicine, 1983; 6: 75.

(4) Alveolar-capillary membrane permeability in radiation lung injury. IH Ahmed, W Logus GCW Man, SFP Man. Proceedings of the Third Annual Heritage Medical Research Days, 1983; 50.

°(5) Reduced radioaerosol clearance in a model of pulmonary fibrosis. IH Ahmed, JW Logus, GCW Man, SFP Man. Am. Rev. Respir. Dis. April 1984, In Press.

*(6) Use of $Na^{-99m}TcO_4$ to explore Cl^- channels in canine airway epithelium. SFP Man, IH Ahmed, GCW Man, A Hguyen. Clinical and Investigative Medicine, 1983; 6: 78.

°(7) The effects of high frequency oscillatory ventilation (HFOV) on alveolar clearance of radioaerosol. IH Ahmed, JW Logus, SFP Man, GCW Man. Am. Rev. Respir. Dis. April 1984, In Press.

(8) Male/female differences in lung aerosol deposition and clearance. HY Yamamoto, IH Ahmed, J Horsley, JW Logus, GCW Man, SFP Man. Proceeding of the Third Annual Heritage Medical Research Days, 1983; 50.

(9) Upper airways obstruction in bulbar poliomyelitis. IH Ahmed, NE Brown. Proceedings of the Alberta Thoracic Society, 1981.

+ Presented at the American College of Chest PhysiciaNs annual meeting in November 1983.

* Presented at the CSCI annual meeting in September 1983.

° To be presented at the American Thoracic Society annual meeting in May 1984.